

On the irreversibility of internal-wave dynamics due to wave trapping by mean flow inhomogeneities. Part 1. Local analysis

By SERGEI I. BADULIN AND VICTOR I. SHRIRA

P. P. Shirshov Institute of Oceanology, Russian Academy of Sciences, Krasikova 23,
Moscow, 117218, Russia

(Received 1 December 1991 and in revised form 15 September 1992)

The propagation of guided internal waves on non-uniform large-scale flows of arbitrary geometry is studied within the framework of linear inviscid theory in the WKB-approximation. Our study is based on a set of Hamiltonian ray equations, with the Hamiltonian being determined from the Taylor–Goldstein boundary-value problem for a stratified shear flow. Attention is focused on the fundamental fact that the generic smooth non-uniformities of the large-scale flow result in specific singularities of the Hamiltonian. Interpreting wave packets as particles with momenta equal to their wave vectors moving in a certain force field, one can consider these singularities as infinitely deep potential holes acting quite similarly to the ‘black holes’ of astrophysics. It is shown that the particles fall for infinitely long time, each into its own ‘black hole’. In terms of a particular wave packet this falling implies infinite growth with time of the wavenumber and the amplitude, as well as wave motion focusing at a certain depth. For internal-wave-field dynamics this provides a robust mechanism of a very specific conservative and moreover Hamiltonian irreversibility.

This phenomenon was previously studied for the simplest model of the flow non-uniformity, parallel shear flow (Badulin, Shrira & Tsimring 1985), where the term ‘trapping’ for it was introduced and the basic features were established. In the present paper we study the case of arbitrary flow geometry. Our main conclusion is that although the wave dynamics in the general case is incomparably more complicated, the phenomenon persists and retains its most fundamental features. Qualitatively new features appear as well, namely, the possibility of three-dimensional wave focusing and of ‘non-dispersive’ focusing. In terms of the particle analogy, the latter means that a certain group of particles fall into the same hole.

These results indicate a robust tendency of the wave field towards an irreversible transformation into small spatial scales, due to the presence of large-scale flows and towards considerable wave energy concentration in narrow spatial zones.

1. Introduction

The problem of describing interactions between internal waves and large-scale oceanic motions, which is crucial in understanding oceanic internal-wave dynamics and energetics is still very far from finally being resolved (e.g. Miropolsky 1981; Olbers 1983; Levine 1983). The present state of internal-wave theory is characterized by the search for the strongest mechanism of interaction, which can lead to considerable energy exchange between waves and currents, internal-wave energy transfer into distant spectral bands, wave breaking, etc.

One such mechanism – the trapping of internal waves which propagate in a guide (horizontally varying due to the non-uniformity of stratification and currents) – was found by Badulin, Shrira and Tsimring (Badulin, Tsimring & Shrira 1983; Badulin, Shrira, Tsimring 1985, hereafter referred to as BST1 and BST2). The essence of this mechanism is as follows. In the framework of linear inviscid theory there are regions of ‘non-transparency’ for comparatively short (typically with wavelengths less than 10^3 m) guided internal waves propagating on non-uniform currents. A wave packet approaches the boundaries of these regions of non-transparency asymptotically, i.e. it tends to stop in a frame of reference moving with the current and the intrinsic wave frequency tends to the maximum frequency of linear internal waves (for example, the maximum value over depth of the Brünt–Väisälä frequency in the model of shearless basic flow). All this enables us to speak about *wave trapping* by the current and to refer to the boundary of non-transparency (for a given wave) as the *wave trapping layer*. (In fact we have a *line* of trapping, but we preserve the ‘historic’ term.) Hereafter we use the term ‘trapping’ in this sense only. It is also often used for waves propagating in a certain wave guide – we shall refer to these waves as ‘guided’ or ‘localized’.

The effectiveness of the wave trapping mechanism and the very fact of its existence were demonstrated in BST1 and BST2 for the simplest type of non-uniformity (the ambient fields of current velocity $U(x, z)$ and stratification $N(z)$ were considered to depend on one of the horizontal spatial coordinates only). We list below some of the results derived within this model. It was shown that when a wave packet approaches the trapping layer, wavenumber and amplitude grow with time while wave motion tends to concentrate at a certain depth. Within the bounds of the linear inviscid theory the growth of wavenumber and amplitude is unbounded.

Firstly, this picture of wave trapping was derived in the WKB-approximation of linear theory. Exact solutions of the model problem (Erokhin & Sagdeev 1985*a, b*) confirm the main conclusions of the approximate theory, including the validity of the WKB-approximation. Some experimental evidence of internal-wave trapping in a strong horizontally inhomogeneous current (Lomonosov current) has been reported recently (Badulin, Vasilenko & Golenko 1990). It has been found that under certain conditions the trapping definitely takes place and produces strong effects like wave breaking or, at least, stimulates small-scale turbulence generation at the depth of maximal stability, i.e. at the maximum of the Brünt–Väisälä frequency. We note that the range of wave and current parameters where the phenomenon has been observed in its simplest form is not so typical of ocean conditions as to imply that the trapping in this form is a widespread phenomenon. We believe that another formulation of this problem is of primary interest: whether the trapping takes place as a general tendency of internal-wave-field evolution and how this tendency reveals itself.

The asymptotic character of the approach of the packet towards the trapping layer in this context means that the internal-wave dynamics becomes principally irreversible even in the inviscid approximation of linear theory (i.e. within the framework of the theory not taking into account, in particular, wave–wave interactions, wave breaking processes or the existence of critical layers).

Let us specify the place of our problem within the vast corpus of recent works, where the term ‘irreversibility’ has been used in the context of internal wave dynamics.

The first group of works worth mentioning here, initiated by McComas & Bretherton (1975), starts with the kinetic equation for the internal-wave field or certain analogues of this equation. Irreversibility in these problems comes from certain ensemble averaging of wave characteristics as in the kinetic theory of gases. This irreversibility is connected with the conservative mechanisms and provides energy

exchange among motions of different scales. For the internal waves these mechanisms are the resonant wave-wave (McComas & Müller 1981; McComas & Bretherton 1977) or wave-current (Watson 1985) interactions. In the latter case, the current is represented by a large-scale wave motion assumed to be stochastic.

Very close to the first group lies the one where both the deterministic and stochastic fields are under consideration (Raevsky 1983; Bunimovich & Zhmur 1986). The typical problem statement is as follows: a wave packet (the deterministic part of the wave field) propagates through a stochastic environment. In this case, 'irreversibility' reflects the scattering of the deterministic component.

'Pure deterministic irreversible' problems can be considered as those dealing with the elementary interactions in an appropriate wave field, that is, as 'bricks' of the problems mentioned above. Commonly, consideration of these problems involves such physical mechanisms as strong nonlinearity (e.g. wave breaking) or wave instability. In particular, the inhomogeneity of ocean currents causes transformation of internal waves in the small-amplitude approximation, and then significant nonlinear and viscous effects become apparent, which in their turn provide 'classical' irreversibility.

Within the 'pure deterministic irreversible' class of problems there is a special group concerned with asymptotic-with-time effects, the most well-known of which is the critical layer phenomenon (e.g. Booker & Bretherton 1967). The number of review works devoted to different aspects of wave dynamics near critical layers is too large to be listed. (For the basic references see the book by LeBlond & Mysak 1979.) In view of recent results, the critical layer should not be considered to be of prime importance for the internal wave field energy balance; earlier overestimations of its role was a consequence of the problem idealization (Borovikov 1988). Other types of wave asymptotic behaviour due to singularities of different natures, including the 'trapping singularity that we are interested in, have been studied by Basovich & Tsimring (1984) and Olbers (1981). In the latter, the relation between critical layer and trapping layer phenomena was demonstrated fairly well. The mathematical difference lies in the statement of the physical problem. Trapping layers and critical layers can be viewed as the two limits of the same problem and their physical models have their own range of applicability. However, in both these important works the approximation of constant Brünt-Väisälä frequency was essential and inhomogeneity of the mean hydrophysic fields was, in fact, one-dimensional.

However, the physical picture of trapping differs significantly in one-, two- and three-dimensional problems. The increase of dimensions changes the mathematical nature of the problem significantly and leads to quite different physical consequences. In particular, the concentration of wave energy occurs in a plane in the one-dimensional problem, in a line in the two-dimensional problem and at one point, according to one of possible scenarios, in three-dimension. Thus, it is fundamental to an understanding of the phenomenon of trapping to analyse the situations where both horizontal and vertical inhomogeneities are important together.

In this paper we pose the question concerning the structural stability of the effect of trapping and the tendency towards irreversible transformation of internal waves to the small scales in mean hydrophysic fields of arbitrary geometry. We have some grounds to suppose that other effects which will not be considered here do not fundamentally change the results of our investigation. For an asymptotical regime of transformation, wave-dynamical irreversibility occurs regardless of the way nonlinearity or viscous effects are specified. The phenomenon of trapping is a high-frequency one (relating to the internal-wave frequency range). That makes the effect, unlike in the critical layer case, structurally stable and therefore important. We recall that as the wave frequency

near the critical layer tends to zero, the wave dynamics becomes strongly influenced by low-frequency variations of the mean current, inertial waves (see e.g. LeBlond & Mysak 1979; Broutman 1986; Broutman & Grimshaw 1988), Earth rotation, etc. An essential feature of wave trapping is that both the vertical and horizontal wave scales tend to zero, while in a critical layer only the vertical scale diminishes, and in problems of wave instabilities the spatial scales, as a rule, remain the same or vary slowly.

While studying general properties of internal-wave dynamics on inhomogeneous currents a number of questions arise in connection with the phenomenon of trapping. The first is whether the tendency of the field of guided internal waves to irreversible transformation into the small-scale band holds when the waves propagate on horizontally and vertically inhomogeneous currents of arbitrary geometry. This question can be paraphrased in terms of questions regarding internal-wave trapping in an arbitrary inhomogeneous ambient current field. In particular, questions about the existence (non-existence) of trapping and relations between the universality of its basic features established in BST1, BST2 and the modification of these features. This work presents some answers to these questions and is organized as follows.

In §2 we give the problem formulation. We start with the known set of Hamiltonian ray equations which describes the propagation of small-amplitude internal waves in a horizontally non-uniform ocean in the WKB-approximation (e.g. Voronovich 1976; Miropolsky 1981). The characteristics of the vertical inhomogeneity (vertical profiles of mean stratification and large-scale current) are incorporated into the Taylor–Goldstein boundary-value problem. Its solution yields the local dispersion relation, i.e. the Hamiltonian of the system.

Thus, within the accepted WKB-approximation the problem of a complete description of the wave-packet dynamics in the non-uniform flow field reduces to solving a set of four Hamiltonian equations. This system describes the motion of a particle-wave packet (with momentum k) in a certain force field. We stress that the structure of this field is determined not only by the dependence of the mean flow on horizontal spatial coordinates, but also by kinematic characteristics (wave vector) of the internal-wave packet itself. The internal-wave dispersion law leads (in terms of the particle-wave analogy) to the occurrence of special singularities of the force field potential ('potential holes'). Some particles 'fall' into these holes for an infinitely long time (each 'type' of particle falls into its own holes), while the particle momentum also grows infinitely. Thus, the trapping layer acts as a specific perfect absorber or, using the astrophysical analogy, as a '*a black hole*'. Hence, the problem of describing the phenomenon of trapping can be formulated as the problem of particle dynamics in the hole neighbourhood. We recall that the infinitely long falling of particles into these holes is interpreted as the waves undergoing an irreversible transformation to small scales. Further we shall study only this specific conservative and, moreover, Hamiltonian irreversibility.

The discussion of the methods and approximations in §2, however, does not touch upon the important questions, which weakly depend on the geometry of the basic flow. Namely, in justifying the validity of the WKB-approximation, the calculation of dissipative and nonlinear effects was not given. These questions have been discussed in detail in BST2 for a plane mean flow. In particular, the validity of the WKB-approximation for a proper description of wave trapping was demonstrated (BST1, BST2). Later this fact was also confirmed by analysing the exact solution for the corresponding 'reference' equation of a linearized problem in the vicinity of the singular point (Erokhin & Sagdeev 1985*a, b*). In these works the importance of viscosity and packet bandwidth for the final stage of the packet evolution was shown

as well. A quantitative description of these factors can be easily provided for arbitrary flow geometry in a similar way. Nevertheless, we confine ourselves to the paradigm of the ideal fluid and the quasi-monochromatic wave, aiming to understand and demonstrate the basic qualitative features of internal-wave dynamics in an inhomogeneous flow field *per se*. We try to achieve this goal by studying a chain of comparatively simple models. The models are chosen so that, on the one hand, they can be analysed in detail, and on the other hand, they are proper ‘bricks’ for the synthesis of a consistent view.

The present paper, which is the first part of the work, is based on an approximation which we refer to as the ‘*local analysis approximation*’. Its essence is an expansion of the Hamiltonian (or straightforwardly the flow field) in power series in the horizontal coordinates. The analysis based on the leading terms of this expansion can be justified for a certain range of spatio-temporal scales and in this sense is ‘local’. The scales of validity are not small owing to the small horizontal gradients of the flow and to the small group velocity of short internal waves. The questions concerning the quantitative evaluation of the validity range and the ‘non-local’ effects, in particular the global behaviour of trajectories, are the subjects of the second part of this work (Badulin & Shrira 1993). We note that the local analysis approximation simplifies greatly the mathematics of the problem.

Section 3 (the main results of which were briefly reported in Badulin & Shrira 1985) is concerned with the model where the basic current is considered to be vertically uniform while the basic density stratification is assumed to be horizontally homogeneous. The main types of internal-wave dynamics are distinguished and quantitatively described. The presence of the flow’s vertical shear drastically complicates the packet dynamics in the case of two-dimensional flow non-uniformity. Still, in §4 we obtain a quantitative description for a number of important models and acquire a qualitative understanding of the general situation. The tendency to irreversibility holds for internal-wave conservative dynamics under rather general conditions.

Section 5 presents a brief discussion of the results and directions of further investigation.

2. Formulation of the problem

2.1. Geometric optics approximation; basic equations

We will study internal-wave dynamics on a steady ambient stratified large-scale shear flow with given $U(U(z, \mathbf{x}), V(z, \mathbf{x}), 0)$ and stratification $N(z, \mathbf{x})$; here \mathbf{x} is the horizontal and z is the vertical coordinate respectively, and $N(z, \mathbf{x})$ is the Brünt–Väisälä frequency. The horizontal scale L of the flow variability greatly exceeds the typical vertical scale d . We shall consider small-amplitude internal waves with wavelength λ much smaller than the characteristic horizontal scale L ($\lambda \ll L$). Under these scale relations we can naturally use the ray optics approach (WKB-approximation) for describing the wave propagation (Miropolsky 1981; Voronovich 1976). Then the wave is supposed to be locally plane with local wave vector \mathbf{k} and absolute (i.e. measured in a laboratory frame of reference) frequency ω . At each point on the horizontal plane \mathbf{x} the dependence of ω on \mathbf{k} , as well as the vertical mode structure, are found by solving the Taylor–Goldstein boundary-value problem

$$(\omega - \mathbf{k} \cdot \mathbf{U})^2 \partial_{zz}^2 w + [N^2 |\mathbf{k}|^2 - (\omega - \mathbf{k} \cdot \mathbf{U}) \partial_{zz}^2 (\omega - \mathbf{k} \cdot \mathbf{U}) - |\mathbf{k}|^2 (\omega - \mathbf{k} \cdot \mathbf{U})^2] w = 0, \quad (2.1)$$

with the standard boundary condition at the sea surface and the bottom. We shall take

homogeneous (zero) boundary conditions. The choice of boundary conditions does not influence our subsequent analysis and results. Here $w(z, \mathbf{x})$ is the vertical wave-velocity component which depends parametrically on the horizontal coordinate \mathbf{x} .

The ray equations

$$\dot{x}_i = \partial_{k_i} \omega; \quad \dot{k}_i = -\partial_{x_i} \omega, \quad (2.2)$$

give us the wave packet coordinates \mathbf{x} and wave vector \mathbf{k} as functions of time t . The evolution of the wave vertical velocity w is governed by the equation of conservation of wave action I

$$I_i + \nabla \cdot (\partial_{k_i} \omega I) = 0, \quad (2.3a)$$

where

$$I = \int_{-H}^{\eta(0)} \{N^2(\omega - \mathbf{k} \cdot \mathbf{U})^{-3} + \frac{1}{2}(\mathbf{k} \cdot \mathbf{U})_{zz}(\omega - \mathbf{k} \cdot \mathbf{U})^{-2} |\mathbf{k}|^{-2}\} w^2 dz \\ + w^2 [g(\omega - \mathbf{k} \cdot \mathbf{U})^{-3} + \frac{1}{2}(\omega - \mathbf{k} \cdot \mathbf{U})_z(\omega - \mathbf{k} \cdot \mathbf{U})^{-2} |\mathbf{k}|^{-2}]_{z=\eta(0)}. \quad (2.3b)$$

Here w is not a normalized eigenfunction as is usually supposed in linear homogeneous problems, but it is determined by initial conditions at a point \mathbf{x}_0 . We shall use the term 'internal-wave amplitude' and notation A for the maximum-over-depth value of the wave vertical velocity w . The last term on the right-hand side of (2.3b) describes the 'direct' influence of the surface boundary conditions. Further, we shall neglect this influence by imposing rigid-lid homogeneous conditions at the free surface and the bottom, or the condition of decaying w at infinite $|z|$.

Thus within the accepted approximations the problem is reduced to that of solving:

- (i) the local Taylor–Goldstein boundary-value problem (2.1) (this gives us the Hamiltonian $\omega(\mathbf{k}, \mathbf{x})$ and the vertical structure of $w(z, \mathbf{x})$);
- (ii) the set of Hamiltonian ray equations (2.2) (this describes the wave kinematics);
- (iii) the transport equation (2.3a) which governs the full spatial dependence $w(z, \mathbf{x})$ and hence the amplitude A .

It should be noted that the three-dimensional problem is now (in the WKB-approximation) split into two independent parts: deriving the local (at each point (x, y)) wave vertical structure via (2.1) and then describing the evolution of the wave parameters (determined by $\omega(\mathbf{k}, \mathbf{x})$ and $I(\mathbf{k}, \mathbf{x})$) in two spatial dimensions. However, even such 'two-dimensionalization' of the three-dimensional problem does not give any hope for its complete analysis in the case of an arbitrary flow, as not only can the dispersion law $\omega(\mathbf{k}, \mathbf{x})$ be rather capricious, but the very problem of deriving it from (2.1) is not generally solvable. The proper choice of a number of somewhat simplified models illuminating the main features of the phenomenon under study and its detailed subsequent analysis seems to be the most natural way forward in this situation. We start by recalling some results derived within the simplest model in BST1 and BST2.

2.2. The phenomenon of trapping in the simplest flow geometry

Consider the simplest model of horizontally non-uniform stratified mean flow

$$N = N(z); \quad U = (U(y), 0, 0).$$

Then, splitting into the horizontal and vertical problems becomes almost complete. In the Doppler relation

$$\omega(\mathbf{k}, \mathbf{x}) - \mathbf{k} \cdot \mathbf{U} = \Omega(\mathbf{k}) \quad (2.4)$$

(ω is the frequency in a laboratory system, Ω is the intrinsic wave frequency in the reference frame moving with the ambient flow) $\Omega(\mathbf{k})$ can be found from boundary-

value problem (2.1) with $U = 0$, that is $\Omega(\mathbf{k})$ is a function with well-known properties and is independent of \mathbf{x} . Let us consider internal-wave kinematics near the point y_{tr} , specified as follows

$$k_0 U(y_{\text{tr}}) = (\omega - N_{\text{max}}), \quad (2.5)$$

where N_{max} is the maximum-over-depth value of $N(z)$ and k_0 is the x -wave-vector component. As a packet approaches y_{tr} , Ω tends to N_{max} and, according to the known asymptotics of $\Omega(\mathbf{k})$, the wavenumber tends to infinity and the y -component of the group velocity decreases so rapidly that it takes an infinite time for the packet to reach $y = y_{\text{tr}}$, i.e. the packet approaches this point asymptotically. This is easily seen from the expression for time τ_1 (τ_1 is the time for the packet with initial wave vector $\mathbf{k}(k_0, l_0)$ to acquire the value $\mathbf{k}(k_0, l)$), which is calculated straightforwardly if we put U_y to be constant:

$$\tau_1 = (l - l_0)/(U_y k_0).$$

According to the known properties of the boundary-value problem, the wavenumber growth causes a transformation of the vertical mode structure: as $|\mathbf{k}|$ grows, the wave motion tends to concentrate at the depth z_m corresponding to the maximum value of the Brünt-Väisälä frequency N_{max} (see figure 1). We refer to this transformation as *vertical focusing* and z_m as *the depth of localization*. We also use the term the *trapping layer* for the vertical plane $y = y_{\text{tr}}$, where the intrinsic group velocity of the packet asymptotically tends to zero. The slowing down of the packet near the trapping layer and zero reflection leads to *spatio-temporal focusing*. All the energy of a monochromatic wave is focused in the immediate vicinity of y_{tr} at the depth z_m . These two factors (spatio-temporal and vertical focusing) cause the infinite growth of wave amplitude near the trapping layer. We stress that this infinite growth is not an artifact of our use of the WKB-approximations, which remains valid here up to the singularity (BST1; BST2). These results were also confirmed later within the framework of exact linear theory (Erokhin & Sagdeev 1985*a, b*).

2.3. Internal waves on a flow with arbitrary non-uniformities: preliminary remarks

The simplicity of the analysis in the previous subsection has mainly been based on the possibility of the easy natural separation of the two wave transformation mechanisms mentioned above, namely, the mechanisms connected with the evolution of the wave kinematic characteristics ('horizontal' factors of transformation) and the factors of the mode structure transformation ('vertical' factors). Commonly, these two classes of mechanism are intricately interrelated and, evidently, an analysis similar to that of the previous subsection is impossible. However, the concepts introduced on this basis (the trapping layer, vertical and spatio-temporal focusing, the depth of localization) prove to be very useful tools for the general case as well.

Some features of internal-wave dynamics in the general case can be more easily understood via the following trick. Let us introduce the effective Brünt-Väisälä frequency N_{eff}

$$N_{\text{eff}}^2 = \frac{N^2(z)(\omega - \mathbf{k} \cdot \mathbf{U}(z^0, \mathbf{x}))^2}{(\omega - \mathbf{k} \cdot \mathbf{U}(z, \mathbf{x}))^2} + \frac{(\omega - \mathbf{k} \cdot \mathbf{U}(z^0, \mathbf{x}))^2 (\mathbf{k} \cdot \mathbf{U}(z, \mathbf{x}))_{zz}}{(\omega - \mathbf{k} \cdot \mathbf{U}(z, \mathbf{x})) |\mathbf{k}|^2}. \quad (2.6)$$

The idea of this trick is an attempt to reduce the problem formally to the case of a vertically uniform current. Let us take a certain arbitrary depth z^0 and define the wave frequency Ω_{eff} in the reference frame moving with the flow at this depth as follows:

$$\Omega_{\text{eff}} = \omega - \mathbf{k} \cdot \mathbf{U}(z^0, \mathbf{x}). \quad (2.7)$$

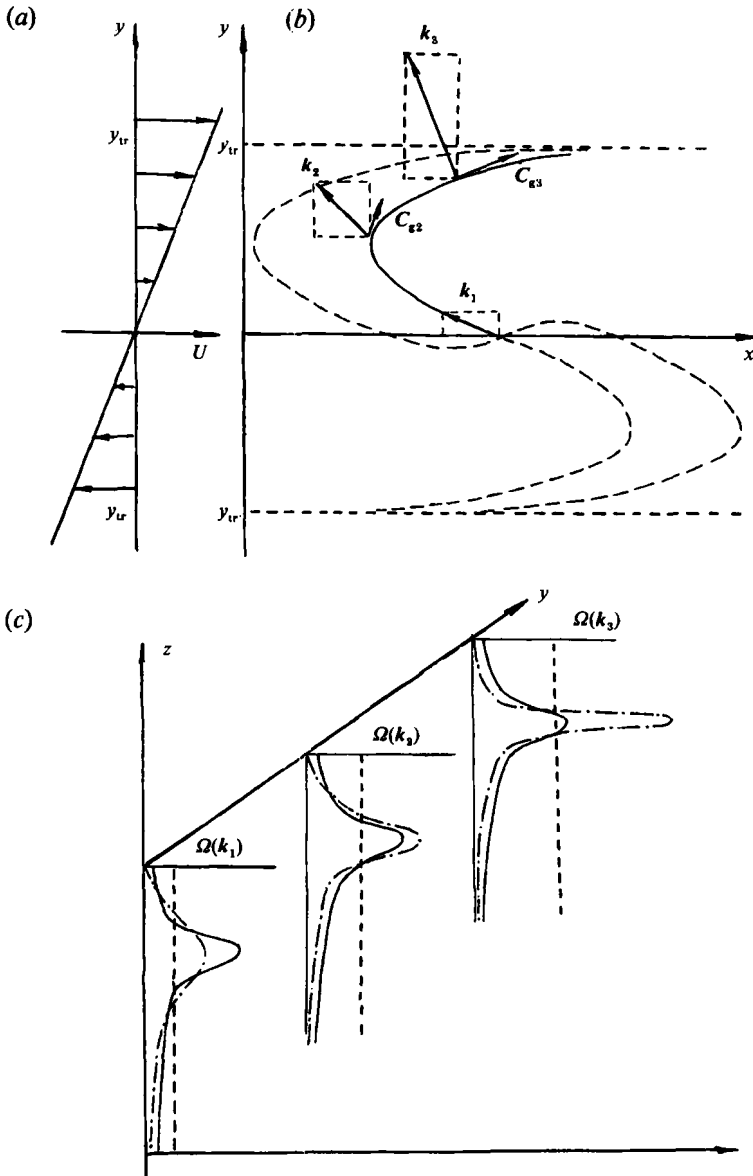


FIGURE 1. The trajectories of a packet trapped by the flow inhomogeneity of the current $U = U_y(0)yi$ and the vertical focusing of a wave trapped by inhomogeneity of the current. (a) The current profile. (b) The trajectories of four packets of the same (modulus) initial (at $y = 0$) frequency and wave vector k projections (k, l). The solid line corresponds to one of the two identical cases (antisymmetric curves) when $k \cdot \partial_y(U)|_{y=0}$ is negative. The unlimited monotonic increase of l (while k remains constant) and decrease of C_{gy} (the y -component of the group velocity C_g) is demonstrated by showing k and C_g at three points (numbered 1, 2, 3) of the trajectory. Near the trapping layer C_{gy} tends to zero; the difference $(C_{gx} - U(y = y_{tr}))$ also tends to zero. Two of the dashed trajectories correspond to packets with positive initial values of $k \cdot \partial_y(U)$. Before the same process of trapping begins these packets should first pass over the simple reflection point (where C_{gy} and l change signs). (c) The profiles of $N(z)$ (solid lines) and of the first-mode eigenfunction $w(z)$ (dot-dashed lines) corresponding to the points 1, 2, 3 of the trapped packet trajectory are plotted. The dashed lines mark the value of the intrinsic packet frequency $\Omega(k)$.

In contrast to the Doppler relation (2.4), here Ω_{eff} explicitly depends not only on \mathbf{k} but also on the horizontal coordinates. Thus, the question of the possibility of the existence of the effect of trapping can be formulated as a question about the way the effective frequency Ω_{eff} approaches or does not approach N_{eff} . Fortunately, to answer these questions it is enough to know only the short-wave asymptote of Ω_{eff} and N_{eff} . The general tool for further study will be the concept of *the effective depth of localization* $z_m(\mathbf{k})$ defined as the depth where N_{eff} reaches a maximum for the given \mathbf{k} .

2.4. Local analysis of internal-wave dynamics

Short internal waves are localized near the depth of localization $z_m(N(z_m) = N_{\text{eff}, m})$. We shall derive the short-wave asymptotics of the boundary value problem (2.1) following a slightly generalized procedure of BST1 and BST2. Expanding the effective Brünt-Väisälä frequency N_{eff} near z_m in powers of $(z - z_m)$, we get the boundary-value problem for the Weber equation

$$w_{zz} + \{ \Pi(z_m(\mathbf{k}, \mathbf{x}, \omega), \mathbf{k}, \mathbf{x}, \omega) + \Pi_{zz}(z_m(\mathbf{k}, \mathbf{x}, \omega), \mathbf{k}, \mathbf{x}, \omega) [\frac{1}{2}(z - z_m)^2] \} w = 0, \quad (2.8)$$

with boundary conditions at infinity

$$w \rightarrow 0; \quad |z| \rightarrow \infty.$$

Here

$$\Pi(z, \mathbf{k}, \mathbf{x}) = \frac{N^2(k^2 + l^2)}{(\omega - \mathbf{k} \cdot \mathbf{U})^2} + \frac{(\mathbf{k} \cdot \mathbf{U})_{zz}}{\omega - \mathbf{k} \cdot \mathbf{U}} - (k^2 + l^2). \quad (2.9)$$

The eigenfunctions $w_n(z)$ of (2.8) corresponding to a discrete spectrum are Hermite polynomials (Abramovitz & Stegun 1964)

$$w(z, \mathbf{k}, \mathbf{x}) = \exp \left\{ -\frac{1}{2} \left(-\frac{1}{2} \Pi_{zz} \right)^{\frac{1}{2}} (z - z_m)^2 \right\} H_n \left\{ \left(-\frac{1}{2} \Pi_{zz} \right)^{\frac{1}{2}} (z - z_m) \right\}. \quad (2.10)$$

The dispersion relation $\omega(\mathbf{k}, \mathbf{x})$ is found from the equation

$$\Pi(z_m(\mathbf{k}, \mathbf{x}, \omega), \mathbf{k}, \mathbf{x}, \omega) \left[-\Pi_{zz}(z_m(\mathbf{k}, \mathbf{x}, \omega), \mathbf{k}, \mathbf{x}, \omega) \right]^{-\frac{1}{2}} = (2n + 1) / \sqrt{2}. \quad (2.11)$$

Using (2.10) and (2.3b) we straightforwardly get the expression for wave action I (for details see BST2)

$$I \approx \int_{-\infty}^{+\infty} N^2 w^2 (\omega - \mathbf{k} \cdot \mathbf{U})^{-3} dz \approx N^2(z_m) A^2 d(z_m) (\omega - \mathbf{k} \cdot \mathbf{U}(z_m))^{-3} \Phi(n). \quad (2.12)$$

Here we suppose U_{zz} to be small and hence the second term on the right-hand side of (2.3b) may be neglected. The third and the fourth terms in (2.3b) are zero when boundary conditions at infinity are used. In (2.12)

$$d(z_m) = \left[-\frac{1}{2} \Pi_{zz}(z_m(\mathbf{k}, \mathbf{x}, \omega), \mathbf{k}, \mathbf{x}, \omega) \right]^{-\frac{1}{2}} (2n + 1)^{-1}$$

is the characteristic vertical scale of mode $w_n(z)$, while $\Phi(n)$ is a universal function of mode number n .

It should be stressed that all the main parameters of short internal waves are thus expressed via (2.9)–(2.12) through the local characteristics of a large-scale flow only. Hence the mechanisms of the short internal-wave transformation to be studied are immediately related to the local spatial structure of the ambient flow (contrary to the case of waves of larger scales), rather than to the integral characteristics of the flow.

Throughout the paper we shall exploit the first-order expansion in the horizontal coordinates of the basic flow

$$\left. \begin{aligned} N(z, \mathbf{x}) &= N_0(z) + N_x x + N_y y, \\ U(z, \mathbf{x}) &= U_0(z) + U_x x + U_y y, \end{aligned} \right\} \quad (2.13)$$

or the Hamiltonian $\omega(\mathbf{k}, \mathbf{x})$ expansion directly. We refer to this first-order expansion as the *local analysis approximation*. Generally, this approximation has a finite temporal interval of validity. The quantitative evaluation of the validity range and 'non-local' effects in wave dynamics will be given in the second part of this work. Here we only note that some 'local' scenarios of trapping can be found within this approximation for which validity of an expansion of the type (2.13) for arbitrary times can be easily confirmed *a posteriori*.

3. Wave dynamics in a vertically homogeneous velocity field

3.1. Internal-wave kinematics

It has already been mentioned (§2.3) that, in the case of vertically homogeneous flow, the problem of finding the dependence $\Omega(\mathbf{k}, \mathbf{x})$ reduces to the analysis of the well-known boundary-value problem for internal waves in a horizontally homogeneous stationary ocean. This allows us to make no preliminary assumptions about the dependence $N(z)$. But for the field $U(\mathbf{x})$ we shall use the local (in the vicinity of some point $\mathbf{x}_0 = 0$) representation (2.13)

$$U = U_0 + U_x x + U_y y, \quad V = V_0 + V_x x + V_y y. \quad (3.1)$$

Rotation of the coordinate system through the angle $\phi = \frac{1}{2} \tan^{-1} [2U_x(U_y + V_x)^{-1}]$ reduces (3.1) to the form

$$U = U_0 + U_y y, \quad V = V_0 + V_x x. \quad (3.2)$$

Here U_y and V_x differ from their values in (3.1); however, we shall use the same notation. For the flow (3.2) a streamline function can be introduced:

$$\Psi = \frac{1}{2} U_y (y + U_0/U_y)^2 - \frac{1}{2} V_x (x + V_0/V_x)^2. \quad (3.3)$$

The streamlines $\Psi = \text{const}$ are the second-order curves (conic sections) and their type is determined by the sign of Δ^2 :

$$\Delta^2 = V_x U_y. \quad (3.4)$$

(In terms of the original variables $\Delta^2 = U_x V_y - V_y^2$).

The remarkable feature of the velocity field approximation considered here is that the system of ray equations splits into two sets of equations that could be solved successively and thus becomes completely integrable. As far as we know, Jones (1969) was the first to notice and exploit this fact. We also mention that approximations of the type (3.2) reveal some remarkable properties which are relevant to nonlinear waves as well and have become the subject of intense studies (Craig 1989; Craig & Criminale 1986).

For the wave vector components we have

$$\dot{k} = -V_x l; \quad \dot{l} = -U_y k. \quad (3.5)$$

We stress that the type of wave evolution (the form of solution of (3.5)) is determined by the sign of Δ^2 only, i.e. by the flow geometry exclusively:

$$\begin{pmatrix} k \\ l \end{pmatrix} = \frac{1}{2} \begin{pmatrix} k_0 - V_x l_0 / \Delta \\ l - U_y k_0 / \Delta \end{pmatrix} \exp(\Delta t) + \frac{1}{2} \begin{pmatrix} k_0 + V_x l_0 / \Delta \\ l + U_y k_0 / \Delta \end{pmatrix} \exp(-\Delta t). \quad (3.6)$$

Consider the behaviour of solutions (3.6) and streamlines $\Psi = \text{const}$ determined by the sign of Δ^2 .

(a) $\Delta^2 = 0$ ('parabolic' point). The velocity is parallel to one of the horizontal coordinate axes. The streamlines are straight. We have considered this case briefly in §2.2 and it has been analysed earlier in detail in BST1 and BST2 and Erokhin & Sagdeev (1985). See also figure 1.

(b) $\Delta^2 > 0$ ('hyperbolic' point, see figure 2a). The streamlines (3.3) are hyperbolas and curves on the plane (k, l) given by (3.6) are also hyperbolas. The asymptotes of hyperbolas $\Psi = \text{const}$ and (3.6) are pairwise orthogonal. It is easy to understand the behaviour of wave-packet trajectories in this case.

We first make a qualitative analysis. Since in the model under consideration the internal-wave intrinsic frequency cannot exceed the maximal value of the Brünt-Väisälä frequency, the Doppler shift (scalar product $(\mathbf{k} \cdot \mathbf{U})$) cannot increase infinitely as $|\mathbf{k}|$ grows infinitely. Therefore, the angle $\chi = \cos^{-1}[(\mathbf{k} \cdot \mathbf{U})/|\mathbf{k} \cdot \mathbf{U}|]$ must tend to $\frac{1}{2}\pi$. Thus, the internal-wave-packet motion in phase space at large times is constituted by the motion of vector \mathbf{k} along the appropriate branch of a hyperbola on the plane (k, l) which is accompanied by 'gluing' of the wave-packet trajectory in the plane (x, y) to a certain streamline. This 'gluing' is caused by peculiarities of the internal-wave dispersion law: namely, the limited value of internal wave intrinsic frequency and, hence, the rapid decrease of intrinsic group velocity with the growth of wavenumber.

As will be shown below, the behaviour of the wave-packet trajectories is qualitatively different for waves of other types with unlimited intrinsic frequencies (surface waves, for example). In this case the trajectories are not glued to the streamlines of the mean flow. The possibility of a concentration of trajectories in the vicinity of a certain curve at large times could lead to infinite growth of wave amplitude.

(c) $\Delta^2 < 0$ ('elliptic' point, figure 2b). The streamlines are ellipses. The wave vector on the plane (k, l) also moves along an elliptic curve oriented at a right angle to the ellipse $\Psi = \text{const}$ on the coordinate plane. In this case there is no tendency to infinite growth of the wavenumber but still a significant wave transformation is possible. Indeed, the ratio of the maximum to the minimum wavenumber is determined by the ratio of velocity shears $\mathbb{R} = |V_x/U_y|^{\frac{1}{2}}$. The large increase of the wavenumber for large values of \mathbb{R} , as well as in case (b), provides conditions for the manifestation of mechanisms of dissipation and nonlinear interaction which are not considered here. This will lead to a 'practically irreversible' type of wave-packet evolution.

3.2. Internal-wave dynamics

Qualitative speculations on the behaviour of the wave-packet trajectories and the possibility of significant growth of wave amplitude can be supported by the exact solutions of the system (2.2)–(2.3).

It is convenient to consider the problem in terms of new variables

$$\zeta_{1,2} = \mathbb{R}x \pm y; \quad \kappa_{1,2} = \frac{1}{2}(k/\mathbb{R} \pm l). \quad (3.7)$$

Indices 1, 2 correspond to the upper and lower signs respectively. Then the solutions to the system of ray equations take the form

$$\kappa_{1,2} = \kappa_{1,2}^0 \exp(\mp \Delta t), \quad (3.8a)$$

$$\zeta_{1,2} = \zeta_{1,2}^0 \exp(\pm \Delta t) + \exp(\pm \Delta t) \int_0^t \exp(\mp \Delta t) \partial \Omega / \partial \kappa_{1,2} dt. \quad (3.8b)$$

When $\Delta^2 > 0$ the axis of the new coordinate frame coincides with the asymptotes of hyperbolic streamlines while κ_1, κ_2 represent components of the 'new' wave vector in this system. Thus, the basis for choosing the new variables becomes clear: we consider

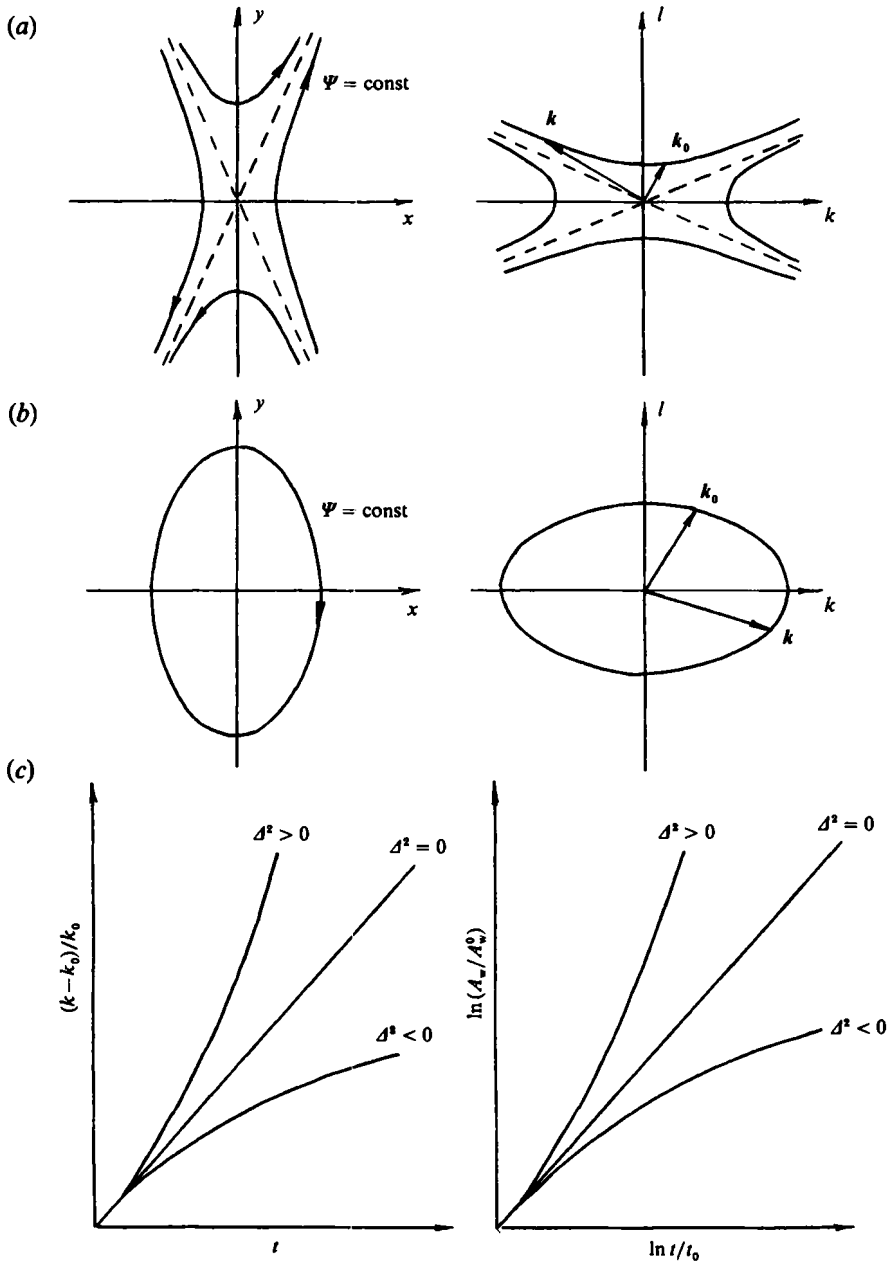


FIGURE 2. Wave-vector evolution depending on the mean current geometry in the 'totally-local' flow field. (a) Hyperbolic streamlines: infinite growth of wavenumber independent of the initial wave parameters (initial wavenumbers and coordinates) and wave type (wave dispersion relation) is depicted in the right-hand sketch. The internal-wave-packet trajectory tends to the streamline (depicted on the left-hand sketch) since the wave group velocity rapidly decreases. While the short-wave packet propagates along the streamline, the wave vector goes along the hyperbola branch which is perpendicular to this streamline. (b) Elliptical streamlines: the wave-vector trajectory is an ellipse (right) and the wave evolution is reversible in k -space (within the framework of linear, nonviscous theory) irrespective of the wave type and wave parameters. (c) Evolution of internal-wave amplitude (right) and wavenumber (left), depending on the mean current geometry (sign of Δ^2): $\Delta^2 < 0$ is the region of reversibility where wave vector and wave amplitude are finite; $\Delta^2 > 0$ is the irreversibility region where wave vector and amplitude grow infinitely with time.

the motion of a wave packet with reference to the asymptotes of hyperbolic streamlines in order to describe properly the effect of the 'gluing' of trajectories to these streamlines.

According to (3.8a) the wavenumber increases exponentially as $t \rightarrow \infty$. The wave front tends to become parallel to asymptotes of hyperbolic streamlines. We note that this type of wave-vector behaviour does not depend on the nature (in this context, on the dispersion relation) of waves propagating upon the shear flow given by (3.1). On the contrary, the form of the dependence $\zeta_{1,2}(t)$ results from the specific features of the wave dispersion law, or, to be more precise, it is described by the behaviour of the integral term on the right-hand side of (3.8b), when $t \rightarrow \infty$. The first term on the right-hand side of (3.8b) describes the wave-packet motion together with the mean flow. Evidently, the behaviour of the second term responds to the intrinsic packet motion relative to the mean flow and allows one to distinguish between two principal possible kinematic regimes for the waves depending on whether the intrinsic group velocity $\partial\Omega/\partial\kappa$ decreases rapidly enough when $|k| \rightarrow \infty$ or not. If not, the term under consideration increases infinitely as, for example, in the case of surface gravity waves. The behaviour of trajectories of internal waves is quite different: the term in (3.8b) describing the intrinsic packet motion has a finite limit when $t \rightarrow \infty$ ($|k| \rightarrow \infty$). The packet covers a finite distance relative to the water mass in which it was originally placed. Short-wave transformation of internal waves in the problem concerned turned out to be local in the coordinate frame that moves with the flow. Thus we can refer to the 'gluing' of trajectories of internal waves to the mean flow streamlines.

It is natural to investigate the relations between internal-wave dynamics and the specific features of wave kinematics mentioned above. From (2.3a) we obtain the law of conservation of wave action I for a stationary case in the form

$$I \frac{\partial(x, y)}{\partial(\xi, t)} = \text{const}, \quad (3.9)$$

where ξ is a parameter of a family of trajectories. Usually ξ is chosen as $x_0(y_0)$. Neglecting the intrinsic packet motion relative to the mean flow we obtain $I = \text{const}$. The increase of packet dimensions along ζ_1 is compensated by its decrease along ζ_2 . Conservation of the packet volume on the (x, y) -plane can be associated with non-divergence of the mean flow.

Thus, the variation of I is due to the intrinsic packet motion relative to the mean flow. From (2.9) in our case we obtain

$$I/I_0 = [1 - \partial\zeta_1^0/\partial\xi(f_2^0(t) - f_2^0(0)) - \partial\zeta_2^0/\partial\xi(f_1^0(t) - f_1^0(0))]^{-1}. \quad (3.10)$$

Here

$$f_{1,2}^0(t) = \frac{1}{A} \left\{ \frac{\partial\Omega}{\partial\kappa_{1,2}} \Big|_{t=0} + \int_0^t \exp(\pm At) \frac{d}{dt} (\partial\Omega/\partial\kappa_{1,2}) dt \right\}$$

(indices 1, 2 correspond to the upper and lower signs, respectively), and the parameter ξ is taken in such a way that the equation

$$\partial\zeta_1^0/\partial\xi(\zeta_2^0 - f_2^0(0)) + \partial\zeta_2^0/\partial\xi(\zeta_1^0 - f_1^0(0)) = 1$$

is satisfied. In these terms the equation of caustics $I_0/I = 0$ can be rewritten in the form

$$(\zeta_1^0 - f_1^0(t)) (\zeta_2^0 - f_2^0(t)) = \mathbb{M}, \quad (3.11a)$$

or in terms of the current packet coordinates $\zeta_{1,2}(t)$,

$$(\zeta_1(t) - f_1(t)) (\zeta_2(t) - f_2(t)) = \mathbb{M}, \quad (3.11b)$$

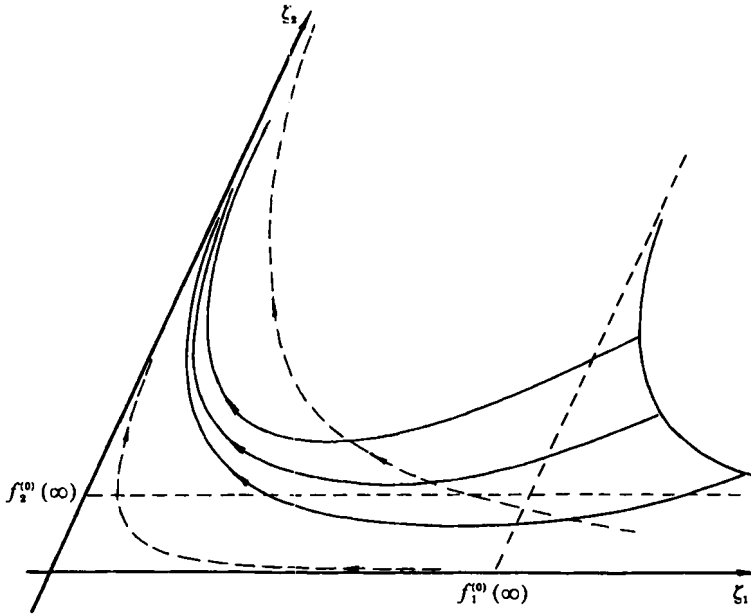


FIGURE 3. Internal-wave-packet trajectories in the case of the irreversible evolution ($\Delta^2 > 0$). 'Unnatural' caustics are formed when time increases infinitely. Trajectories tend to the caustic line asymptotically. Trajectories which started from a hyperbola (solid line) 'glue' themselves asymptotically to the same hyperbola (with the same focal parameter) transferred parallelly (dashed hyperbola). The location of the 'initial' hyperbola determines the parallel shift of the caustic line (mean current streamline) as $\zeta_1 = f_1^0(\infty)$, $\zeta_2 = f_2^0(\infty)$.

where $f_{1,2} = 1/\Delta \partial\Omega/\partial\kappa_{1,2}$ and the constant \mathbb{M} is determined by the initial parameters of the wave packet.

Using the system (3.11a, b) the behaviour of the caustic surfaces can easily be analysed. Let the wave vector $\kappa^0 = (\kappa_1^0, \kappa_2^0)$ be fixed and let us assign a certain value to t . Thereby, as is seen from (3.11b), we will determine the centres of hyperbolas (3.11a, b). Let the wave packet be located at the point $\zeta^* = (\zeta_1^*, \zeta_2^*)$. Having specified the constant \mathbb{M} as

$$\mathbb{M} = (\zeta_1^* - f_1^0(t))(\zeta_2^* - f_2^0(t)),$$

we prescribe a certain spatial cross-section of the ray tube. Rays with the initial wave vector κ^0 , originating from this cross-section, will be focused at moment t on the hyperbola determined by (3.11b). Varying the constant \mathbb{M} , we can represent the whole wave packet in the form of the superposition of its cross-sections by hyperbolas (3.11a) at the initial moment, as well as by superposition of caustic surfaces at an arbitrary subsequent moment t .

Plotting the curves in the way shown in figure 3 is adequate for the case of an ordinary caustic and provides a qualitative explanation of the wave amplitude limitation in the vicinity of an ordinary caustic: spatial 'smearing' of the initial conditions (or finite packet spectrum width) results in the spreading of the caustic surface.

In the present problem the formation of caustics of quite another type occurs when $t \rightarrow \infty$ owing to the aforementioned peculiarity of the internal-wave dispersion relation. For internal waves, as can easily be seen from (3.11a, b), such caustics exist and are associated with the mechanism of 'gluing' of trajectories to the streamlines. In this case for caustic surfaces we have

$$\zeta_1 \zeta_2 = \mathbb{M}. \quad (3.12)$$

The family of hyperbolas (3.12) is one-parametric, contrary to the multi-parametric family (3.11 *a, b*) in the case of ordinary caustics. This means that the explanation of the mechanism of wave-packet amplitude limitation for ordinary caustics given above cannot be applied in the literal sense to the case of caustics formed when $t \rightarrow \infty$.

Making use of (3.3), (3.12) it is not difficult to obtain the asymptotic (when $t \rightarrow \infty$) laws of growth of the wave amplitude A :

$$A \sim \exp\left(\frac{3}{4} \Delta t\right). \quad (3.13)$$

In the case of closed streamlines (the ‘elliptic’ case) the dynamics of internal-wave packets can be considered in a manner quite similar to the case of $\Delta^2 > 0$. The fundamental difference between them lies in the fact that only ordinary caustics are possible when $\Delta^2 < 0$ and the finite value of t corresponds to them through the system of equations (3.11 *a, b*). The qualitative behaviour of the wave amplitude and wavenumber is depicted on figure 2(*c*).

Note that while the evolution of the packet wave vector is of periodic character, the trajectory on the coordinate plane is aperiodic and has the form of an intricate spiral. When $t \rightarrow \infty$ the packet tends to infinity in x -space. Thus, the local analysis of the elliptic case remains valid only for a limited time interval.

3.3. Degenerate case of internal-wave dynamics in a vertically homogeneous velocity field

Within the framework of the model considered here we studied the specific features of internal-wave dynamics. First, we have to pay attention to the structural stability of the effect of ‘gluing’. This structural stability, of course, can disappear in less idealized models. However, the opposite happens to be true: the structurally unstable regime of motion in the model presented here could correspond to a robust physical mechanisms of wave transformation.

Consider trajectories with initial conditions $\kappa_1^0 = 0$, $\kappa_2^0 \neq 0$, $\zeta_1^0 = 0$, $\zeta_2^0 \neq 0$, when $\Delta^2 > 0$. These initial conditions determine the motion along the separatrix of the saddle generated by the streamlines of the mean flow. In this case the wavenumber also grows infinitely and the internal-wave packet asymptotically approaches the saddle point located at the coordinate origin (see figure 4 and its caption). This phenomenon proved to be similar to that of ‘trapping’. Note, however, that in the case considered here the asymptotic approach of the packet to the coordinate origin can occur not only for internal waves, but also for surface gravity waves (see (3.8*b*)) (the group velocity should decrease with the wavenumber growth).

A remarkable new feature should be pointed out: all harmonics asymptotically approach the saddle point, i.e. all spectral components of wave packets focus at one point, and, therefore, dispersive spreading is not able to weaken possible strong dynamic effects which result from the packet trapping. We shall refer to such a phenomenon as *non-dispersive focusing*. The asymptote for internal-wave amplitude similar to (3.13) can easily be found:

$$A \sim \exp\left(\frac{3}{4} \Delta t\right). \quad (3.14)$$

If we give up our assumption that the basic flow has zero divergence, then the structurally unstable situation in the model represented here becomes of true physical interest. In the real ocean there often exist weak vertical motions that lead to divergence of the horizontal velocity field. The simplest model of such flow is the longitudinally non-uniform flow $U = U_x xi$, that corresponds exactly to the case just considered of motion along the separatrix.

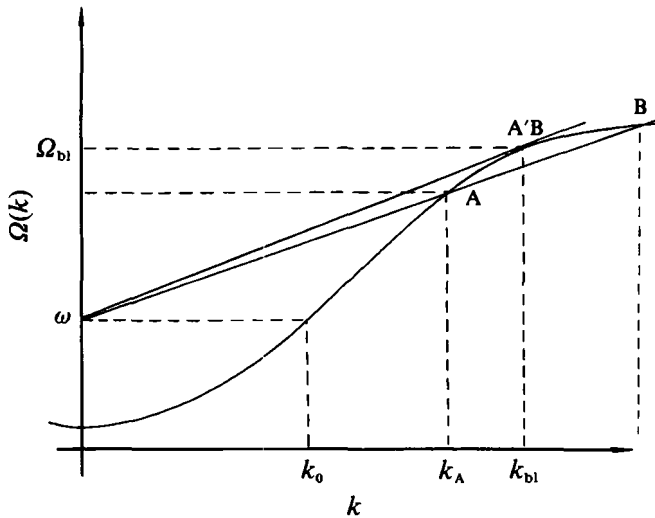


FIGURE 4. The 'longitudinal' trapping of waves on the mean current. The wave with initial intrinsic frequency $\Omega = \omega$ (when $U = 0$) propagates against the mean horizontally inhomogeneous current, varying its kinematic parameters according to the formula: $\omega = \Omega + kU = \text{const}$. Points A, B give its parameters at the intersection of functions $\Omega = \Omega(k)$ and $\omega - kU$ (the Doppler-shifted frequency). Before the junction point of these two solutions the wave parameters are determined by the point A. Then point B gives the wave evolution. The sign of the group velocity changes and the wave travels to the point $U = 0$. As wavenumber grows, infinitely, group velocity tends to zero, and it takes an infinitely long time for the packet to reach the point where $U = 0$.

3.4. Conclusions

In discussing the results of this section we would like to dwell upon some points which are important for subsequent analysis.

Applying the local analysis approximation to internal-wave dynamics we have distinguished and described two basic types of wave-packet evolution on horizontally non-homogeneous flows:

- (i) irreversible inviscid transformation of internal waves into the region of small horizontal and vertical scales (models *a*, *b* of §3.1 - $\Delta^2 > 0$);
- (ii) reversible transformation, i.e. with quasi-periodic time variation of packet kinematic parameters ($\Delta^2 < 0$).

A specific type of evolution in our models is determined by the mean flow field structure only (namely, by the sign of Δ^2). What is the physical meaning of this relation? Using the geometric optics approximation accepted here it is natural to consider the internal-wave propagation as the motion of packet particles in a certain force field. The motion of such particles is determined by the force-field structure and particle inertia. Depending on the relationship between these factors, i.e. the properties of the particles and the force field, effective acceleration of the particle (growth of wavenumber momentum) may or may not take place. The specific features of an internal-wave-packet particle is that its 'acceleration' (trapping), as was found in this section, takes place under rather general conditions and we stress that it does not depend on particle characteristics.

We emphasize one more important feature of internal-wave particles. At large values of the wavenumber, internal waves have so little 'inertia' that the 'gluing' of packet trajectories to the streamlines of the mean flow becomes possible. The 'gluing', as far as the internal waves are concerned, is particularly interesting in connection with the possible manifestation of strong dynamic effects, investigation of which is beyond the

scope of this paper. We stress also that the 'gluing' is an important qualitative concept that will be used for the further analysis of more complicated situations.

We also note that the exponential temporal growth of the amplitude of the trapped waves does not mean instability of these disturbances of the ambient flow in the commonly accepted sense of the term (i.e. as an unlimited growth of the energy of disturbances). In our case the energy of the packet continues to be finite during the course of evolution, the unlimited growth of the amplitude being caused mainly by wave energy transfer into another spectral range.

4. Internal waves in three-dimensionally non-uniform shear flows

4.1. Formulation of the problem

To understand when and how trapping occurs in three-dimensional flows in generic situations one should analyse the properties of a dynamical system generated by the four ordinary equations (2.2) with an implicitly given Hamiltonian (via (2.1)). The complete answer requires knowledge of all the trajectories for given arbitrary flow. This task lies far beyond the capabilities of modern theory of dynamical systems. Even if it were possible, the subsequent problem of separating the different mechanisms contributing to this picture would also be a formidable problem. The accepted approximations ('local analysis' and short-wave approximations) which are, in fact, expansions in $|k|^{-1}$ and x , although they simplify the problem greatly, still do not provide a general solution in generic situations.

We confine ourselves to considering a model flow with the form

$$U = yF_1(z), \quad V = xF_2(z), \quad N = N(z) \quad (4.1)$$

(F_1, F_2, N are arbitrary functions of depth z). (The model (3.1) of §3 is a particular case of the model (4.1).) This flow satisfies the Euler equations for a non-rotating ideal fluid and allows a wide class of flow variations within the model. The first-priority questions are: to identify the basic physical mechanisms governing internal-wave propagation in flow (4.1), and to clarify the role of the vertical structure of the current specified by the functions F_1, F_2 and the stratification profile given by $N(z)$.

Consider a short-wave equation of the internal-wave dispersion relation (Borovikov & Levchenko 1987).

$$\omega = \min A \max [N(z) + k \cdot U(z)] + O(|k|^{-\rho}) \quad (4.2)$$

where ρ is a positive value which will be specified below for particular models. As it was pointed out in §2.3 short-wave evolution is determined predominantly by the local hydrodynamic field structure at a certain depth z_m , which corresponds, according to (4.2), to the extremum of the expression in square brackets. Depending on the type of stratification, three different situations occur: z_m is determined mainly by the density stratification $N(z)$; z_m is determined by the current profile $U(z)$; z_m depends on both factors.

We note also that z_m depends upon $U(z)$ only in the combination $(k \cdot U)$. Thus z_m also depends on the wave parameters, via $(k \cdot U)$. In the previous section we dealt with an example of a situation with z_m being fixed, (i.e. z_m did not depend upon the wave parameters). Besides the case of §3, where z_m corresponds to the maximum of $N(z)$, from (4.2) one can easily see other examples of this kind, e.g. z_m corresponding to the ocean surface or the bottom. To describe wave kinematics in the cases with z_m independent of k , one can repeat all the results of §3, inserting $U(z_m)$ into all expressions in place of U .

Here we shall concentrate our attention on another class of situations, namely those where z_m strongly depends on k and the wave dynamics is therefore much more complicated. Distinguishing the influence of stratification and of shear upon z_m as different mechanisms governing the wave-guide parameters, one should bear in mind that the prevalence of one or other mechanism is determined either by the specifics of the vertical structure of the given flow, or by the wavenumber range under consideration. By varying the flow structure and the wave scales within the bounds of the model (4.1) we shall elucidate the basic features of guided internal-wave dynamics in shear flows.

4.2. The general properties of the model (4.1)

The main advantage of the model flow (4.1) is the additional symmetries in the ray equations (2.2) in the short-wave limit, which greatly simplifies the study. In particular, the depth of localization z_m (given by (4.2)) appears to be a function of the two new independent variables a ($a = ky$) and b ($b = lx$) only. Thus, the short-wave expansion of the Hamiltonian takes the form

$$\omega = \omega_0(a, b) + o(1). \quad (4.3a)$$

In the general case, z_m and ω_0 are functions of four arguments: x, y, k, l . This symmetry also yields an additional first integral of motion S

$$S = kx + ly. \quad (4.3b)$$

It should be stressed that the specific form of S does not depend on the functions F_1 , F_2 and N (within the model (4.1)). This remarkable fact enables us to find general properties of the wave dynamics within this model.

Taking S and one of the variables a or b as new canonical momenta we can perform a canonical transformation. In Appendix A we give four basic types of this transformation. In terms of these new variables new canonical momenta Q_i (here the indice is the number of the type of transformation in (A 1)) are cyclic. One can also exploit this fact and decrease the number of conjugated variables down to a single pair. Still, we prefer to use the variables of the type (A 1), which do not depend on the specifics of F_1 , F_2 or N .

In terms of these new variables the set of ray equations in the short-wave limit takes the form (see Appendix A)

$$\dot{S}_i = 0, \quad \dot{Q}_i = \partial\omega_0/\partial S_i, \quad (4.4a)$$

$$\dot{E}_i = -\partial\omega_0/\partial Q_i, \quad \dot{R}_i = \partial\omega_0/\partial R_i. \quad (4.4b)$$

We have neglected here the intrinsic wave motion, but the wave kinematics are not trivial here because of the dependence of the depth of localization z_m on the wave vector. Thus in the short-wave limit we have reduced the fourth-order system to a second-order one. Moreover, the zeroth-order Hamiltonian $\omega_0(a, b)$ is the first integral of the system (4.4) with parametric dependence on S_i and our model can be analysed in detail. There are two qualitatively different regimes in the cases of closed/unclosed curves $\omega_0 = \text{const}$ on the (a, b) -plane. Closed curves $\omega_0 = \text{const}$ correspond to time-periodic motion (in terms of a and b , and hence, in terms of Q_i, R_i defined by (A 1)).

The general solution of the ray equation can easily be found in terms of the original variables, using the new variables (A 1) as follows:

$$k = k_0 \exp\left(-\int_0^t \Delta_1 dt\right), \quad x = x_0 \exp\left(\int_0^t \Delta_3 dt\right), \quad (4.5a)$$

$$l = l_0 \exp\left(-\int_0^t \Delta_2 dt\right), \quad y = y_0 \exp\left(\int_0^t \Delta_4 dt\right), \quad (4.5b)$$

where $\Delta_i = \partial\omega_0(E_i, R_i, S_i)/\partial S_i$. For the periodic motion in (a, b) there is a periodicity of the integrals in the exponents in (4.5a) and (4.5b):

$$\int_t^{t+T} \Delta_1 dt = \int_t^{t+T} \Delta_2 dt = \int_t^{t+T} \Delta_3 dt = \int_t^{t+T} \Delta_4 dt. \quad (4.6)$$

Here t is an arbitrary moment of time and T is the period of the motion in the (a, b) -plane. Note that solutions (4.5a, b) look like solutions (3.6) for shearless flow but integrals over period T in (4.6) are evidently not zero and hence strictly periodic motions in the model under consideration are not structurally stable.

One can draw some qualitative conclusions using the notion that flow streamlines in each horizontal cross-section are the second-order curves, together with the result of the previous section. We recall that the canonical variables Q_i are tangents of the angles between the wave (or radius) vector and one of the coordinate axes. Thus periodic variation of a and b leads to a periodic variation of Q_i as well. This means that a certain fixed range of angles is passed by a packet in the same time interval.

Let the packet motion be determined by the flow at two fixed depths z^* and z^{**} . Within the angular intervals $(0, \phi)$ and $(\pi, \pi + \phi)$ the packet moves at the z^* depth and within the angular intervals (ϕ, π) , $(\pi + \phi, 2\pi)$ at the z^{**} depth. Let the flow streamlines at z^* and z^{**} be, for example, ellipses with different parameters. The packet evolves in accordance with (4.5), where instead of U and N , their values at z^* (or z^{**}) are taken. In contrast to the case of the previous section, the wavenumber does not evolve periodically, but grows (or decreases) with every cycle. The wavenumber growth (decrease) with time averaged over the cycles is exponential. The packet trajectories are composed of the flow streamlines at z^* and z^{**} (see figure 5a). One can easily show that helixes of these trajectories will twist (untwist) exponentially as well. These conclusions also hold qualitatively when the next-order terms in the Hamiltonian are taken into account. Owing to the intrinsic packet motion, drift that is linear with time adds to the zeroth-order motion along the streamlines.

The physical interpretation of the relations (4.6) given above can also be applied to cases with more than two depths of localization z_m and where the flow streamlines are not necessarily closed. Figure 5(b) and 6 illustrate this case.

Thus the principal difference between the simplest model of previous section and the model under consideration lies in the effect of variation of the depth of localization z_m .

Before turning to the study of concrete models we would like to fix some general properties of the wave dynamics.

First, we stress again the principal role of the $z_m(\mathbf{k})$ -dependence in the packet evolution. In shearless flows the type of wave evolution is determined for all the packets exclusively by the sign of the universal value Δ^2 , which is prescribed by the mean flow's horizontal gradients and does not depend on the stratification's vertical structure $N(z)$. In shear flows an analogue to Δ^2 also occurs, namely Δ_{eff}^2 . This is the same combination of the flow's horizontal gradients, but taken at different levels z_m . In its turn z_m is a function of \mathbf{k} and of the vertical structure U and N . Thus, the type of packet evolution in the shear flows is determined not only by the flow's horizontal gradients but by the flow's vertical structure and by the initial wave vector and position of the packet.

Second, we note that periodic regimes in shearless flows turn out to be structurally unstable, when the presence of the shear is taken into account.

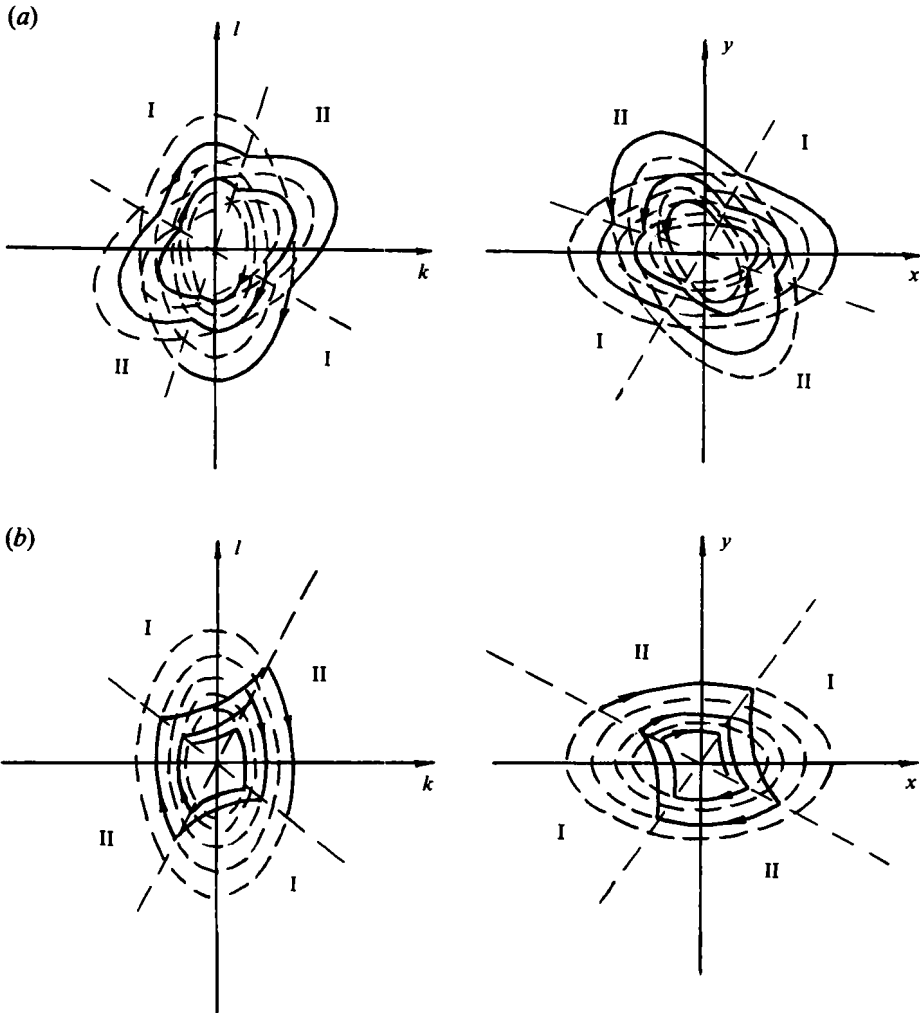


FIGURE 5. Short internal-wave kinematics in the two-depths-of-localization model. Streamlines (dashed-lines) are (a) elliptical over the two depths or (b) elliptical at depth II and hyperbolic at the depth I. Short internal waves propagate along the streamline of the first depth in the sectors I and along the streamline of the second depth in the sectors II (its trajectory is the solid line). For the wave packet to come back to the same streamline it started from, a certain relation between the parameters of these ellipses (or ellipse and hyperbola) of regions I and II should be strictly satisfied. This does not occur in the general situation when the wave trajectories (in the x -plane or in the k -plane) are not closed and the wave-packet parameters grow (decrease) parametrically. For the model discussed, sectors I and II are fixed for the different wave vectors. Thus, the type of wave evolution (reversible or irreversible) is determined by the current geometry only. In the irreversible case when wavenumber grows infinitely, the wave packet tends to the point $x = 0$, $y = 0$. Then the local approximation is adequate for this model.

4.3. Internal waves in the ocean with prevailing vertical non-uniformity of density stratification

In the previous subsection we found out some general properties of the model (4.1) and showed how to interpret them on the basis of concepts derived in §3 for shearless flows. We proceed now to study concrete models to distinguish characteristic regimes of short-wave transformation in certain 'basic' types of flow vertical structure.

We start with the problem which seems to be a natural continuation and extension

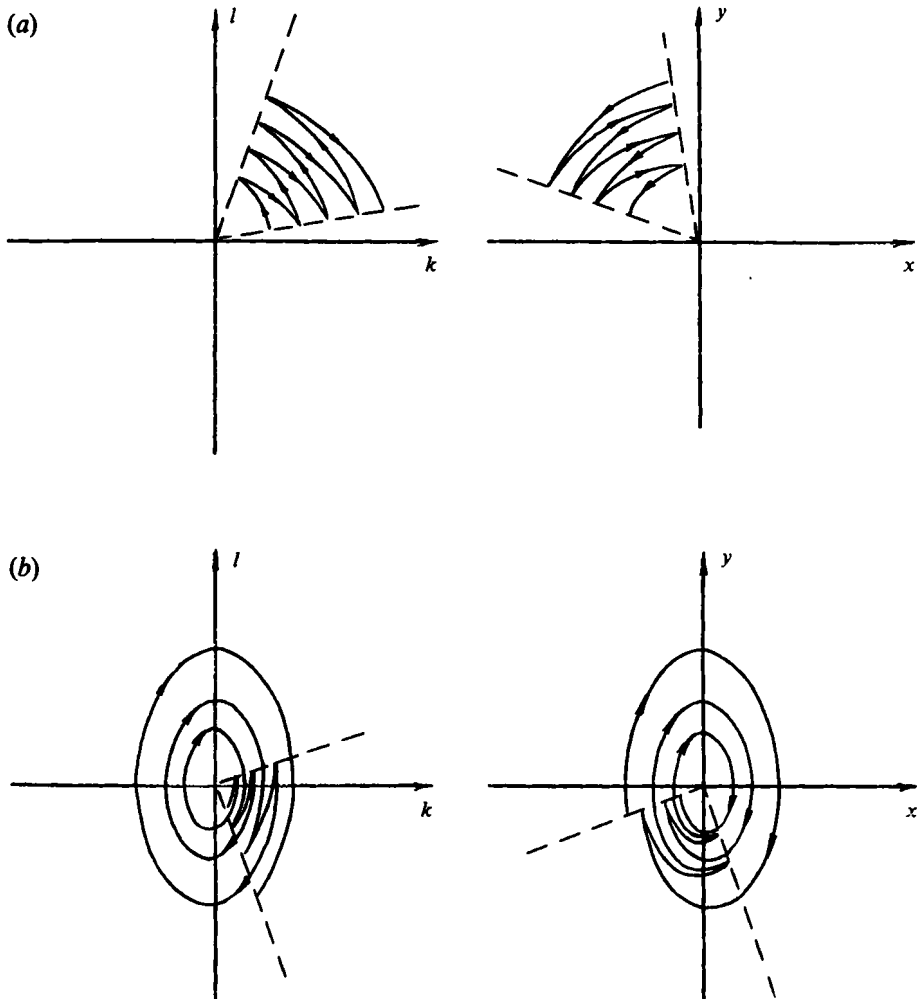


FIGURE 6. Examples of short internal-wave trajectories (in the x - and k -planes) described by the model (4.1). The trajectories may (a) fill sectors in the x - and k -planes, or (b) propagate throughout the whole angle range. Since the localization depth depends on the wave parameters (wave-vector and wave-packet coordinates) these sectors and the type of wave evolution are not solely determined by the mean-current field geometry. The trajectories in this model twist or untwist exponentially.

of the model of shearless flow (3.1). According to (4.2) the wave guide in the short-wave limit is determined by the velocity shear structure. On the other hand, the vertical non-uniformity of stratification usually dominates in the real ocean. That is why the question about ‘transient’ regimes (from one dominating factor to another) is of interest.

4.3.1. Wave kinematics in the model with constant vertical shear

Consider a particular case of (4.1):

$$U = Ay(1 + \alpha(z - z_1)), \quad V = Bx(1 + \beta(z - z_2)), \quad N^2 = N_0^2(1 - \frac{1}{2}\gamma^2 z^2). \quad (4.7)$$

The constants α , β and γ in (4.7) prescribe inverse vertical scales of the flow variability. In this case a wave guide exists owing to the presence of the maximum $N(z)$. The presence of mean shear only shifts its position. That is why we refer to the flow (4.7) as an example of a model with the role of density stratification prevailing.

It is easy to obtain all the kinematic parameters in the short-wave approximation using the results of the previous discussion (see Appendix B). The expression for z_m demonstrates the main qualitative features of all shear flows mentioned above: dependence of the depth of localization on wave parameters. In the short-wave limit

$$z_m^\infty = \pm \sqrt{2/\gamma}. \quad (4.8)$$

The sign of z_m^∞ is determined by the initial wave parameters, namely by the sign of the first integral of motion S . The leading term of the Hamiltonian ω_0 depends on S in a similar way. This is also true for the next-order term of the Hamiltonian, ω_1 . Thus we can illustrate the properties of the system (4.1) generated by parametric dependence of ω_0 on S , using the model (4.7) as the simplest example.

In the short-wave limit the problem of describing the wave kinematics reduces to the case studied in detail in §§3.1 and 3.2. The type of wave evolution is determined by the flow geometry at the corresponding depth. The value

$$A_{s\pm}^2 = AB[1 - \beta(z_2 \pm \sqrt{2/\gamma})][1 - \alpha(z_1 \pm \sqrt{2/\gamma})] \quad (4.9)$$

prescribes the type of wave evolution in the same way as A^2 in the case of shearless flow.

The existence of the two different wave guides can generate some interesting qualitative effects. Consider flows where

$$A_{s+}^2 A_{s-}^2 = A^2 B^2 [(1 - \beta z_2)^2 - 2\beta^2 \gamma^{-2}] [(1 - \alpha z_1)^2 - 2\alpha^2 \gamma^{-2}] < 0. \quad (4.10)$$

Then, wave evolution in one wave guide will be reversible, while in the other one it will be irreversible. For an oceanic seasonal thermocline, typical vertical scales of current variability often exceed those of stratification, i.e. in terms of the scales α , β and γ , $(\alpha^2 + \beta^2) \ll \gamma^2$. Under this condition the inequality (4.10) reduces to a realistic assumption that one of the current velocity components is small at the pycnocline. Then the wave propagating in one direction (with S positive) will be trapped, while the wave with negative S will not. This can cause noticeable anisotropy of the wave field.

4.3.2. Internal-wave dynamics in stratified flows with constant vertical shear

Wave dynamics within the model (4.7) can be treated in a very similar way to the case of §3.2. Non-trivial features of the dynamics are mainly caused by vertical redistribution of the wave energy. Here we shall discuss qualitative features of the internal-wave dynamics. Some formulae are given in Appendix C.

The presence of the vertical shear of the mean current changes short-wave asymptotes of the dispersion relation and eigenfunctions principally. So, these asymptotes do not tend to those of §3.2 when $\alpha \rightarrow 0$, $\beta \rightarrow 0$. This is an additional illustration of the principal importance of taking the presence of even weak shear into account for wave dynamics in the short-wave limit.

Infinite growth of the wave amplitude is caused both by a vanishing of the Brünt-Väisälä frequency at the depth of localization and by a faster decrease of the wave's vertical scale than in the shearless flows in §3.2 (wave vertical focusing). The simplest asymptotic procedure gives an expression like (3.11 *a, b*) for caustics:

$$\frac{\partial(x, y)}{\partial(\xi, t)} = [f_2 A_s t - (\zeta_2^0 + \epsilon_2/A_s)] \partial \zeta_1^0 / \partial \xi [f_1 A_s t - (\zeta_1^0 + \epsilon_1/A_s)] \partial \zeta_2^0 / \partial \xi = 0. \quad (4.11)$$

Here f_1 and f_2 are functions (§2) of the initial wave parameters and mean flow characteristics only, quite similar to f_1 and f_2 in §3.2. The expressions for ϵ_1 , ϵ_2 as functions of α , β , γ are too cumbersome to write here. It seems that only ordinary caustics (at finite values of t) can exist in this case. As $t \rightarrow \infty$ the wave-packet 'volume' grows linearly in the (x, y) -plane and this causes a function-amplitude decrease.

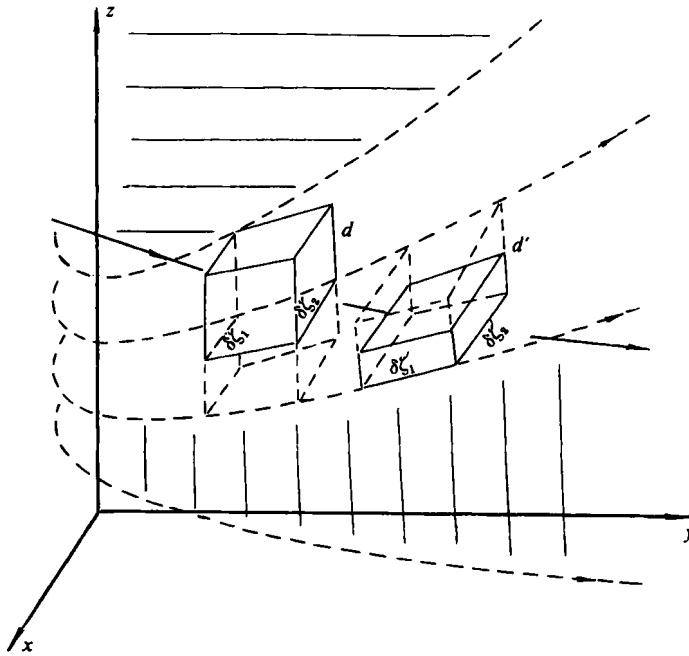


FIGURE 7. The refraction mechanism of internal waves which are trapped by the three-dimensional current. While the depth of the internal-wave localization depends on the wave parameters (its wave vector and frequency) different wave-packet spectral components are 'glued' to the mean current at the different depths. Only dispersion of the wave energy, but not its focusing, may occur in this case. The volume of the wave packet (phase volume in coordinate space) is shown by solid lines. This volume is determined by the streamlines (dashed) to which the wave-packet's harmonics are 'glued' and the dispersive diffusion of the packet.

Figure 7 gives a sketch of this effect. Each spectral component has its own limiting streamline, at its own depth of localization. As the streamlines at the two neighbouring depths diverge infinitely in our model, different harmonics 'glued' onto their own streamlines diverge too. This can be considered as a shortcoming of the model (4.7). The ray family in figure 7 is shown in the case when the depth of localization is a function of the wave parameters. Dotted lines are streamlines at different depths and the bold line depicts the packet trajectory in the (x, y) -plane and the change of depth of its localization. Note that in the model under consideration the dependence of the depth of localization $d(z_m)$ is in the second term ω_1 of the Hamiltonian (see Appendix B). Hence the variation of $d(z_m)$ is a relatively weak effect of the same order as the intrinsic motion of the wave packet.

Some of the properties of wave dynamics derived here are artifacts of the model.

Actually, the processes of interest are localized at the periphery of the pycnocline, where $N \rightarrow 0$. In typical ocean conditions with strong stratification the wave-amplitude growth due to z_m pushing out to the periphery of the pycnocline is obviously limited. Thus, the expressions given in Appendix C have a clear physical meaning of intermediate asymptotics and, therefore, we can use them for a qualitative description only. The asymptotics (C 4) show the direction for further development of our models.

We conclude that vertical focusing of wave motion at a particular depth is the principal determinant of the internal-wave dynamics in the case of arbitrary flow. Other mechanisms, as we have seen, can dominate at the intermediate stage of trapping. Thus we come to the necessity to consider models in which wave propagation depends on the vertical inhomogeneity of the mean shear.

4.4. Internal waves in the ocean with dominant vertical mean flow inhomogeneity

The key result of the previous §4.3 is the principal influence of the variation of the depth of localization on the dynamics of short internal waves. This influence may be weak when a vertical inhomogeneity of density stratification prevails and it vanishes when intrinsic motion of wave packet is neglected. The artifacts of the model discussed above make it necessary to consider advanced models. With more realistic features of the waveguide (for example, buoyancy frequency does not tend to zero) these models can show new physical effect of fundamental importance: the variation of the depth of localization occurs in the short-wave limit when the intrinsic motion of a wave packet is neglected. Further, we shall discuss one of the models of this type:

$$U = Ay(1 + \frac{1}{2}\alpha^2(z - z_1)^2), \quad V = Bx(1 + \frac{1}{2}\beta^2(z - z_2)^2), \quad N = N_0 = \text{const.} \quad (4.12)$$

Here constants $A, B, |\alpha|, |\beta|$ have a similar sense as in (4.7) (α^2, β^2 can be negative). For the depth of localization we get

$$z_m = \frac{\alpha^2 A a z_1 + \beta^2 B b z_2}{\alpha^2 A a + \beta^2 B b}, \quad (4.13)$$

z_m is the key parameter for our problem. We shall concentrate our further discussion on this characteristic. Expressions for the other characteristics are given in Appendix D.

4.4.1. The behaviour of the depth of localization

The specific feature of the model (4.12), unlike the model (4.7), is that the depth of localization's dependence on the wave parameters appears in the short-wave limit. In our model $d(z_m)$ depends on the two variables a and b only. The curves $\omega(a, b) = \text{const}$ which determine the variation of the depth of localization are the second-order curves and, hence, the system can easily be analysed. We shall confine our analysis to qualitative illustrations.

The type of the curves $\omega(a, b) = \text{const}$ depends on the sign of

$$\Delta_{ab}^2 = \alpha^2 \beta^2 - \frac{1}{4}(\alpha^2 + \beta^2 + h^2)$$

exclusively (i.e. on the vertical inhomogeneity parameters only). From the evident inequality $(kx - ly)^2 \geq 0$ in the (a, b) -plane we have

$$S^2 \geq 4ab. \quad (4.14)$$

The inequality (4.14) gives us 'transparency zones' for a harmonic with fixed S . A wave packet moves in the (a, b) -plane along the segments of the curve $\omega_0(a, b) = \text{const}$ bounded by the points of intersections of this curve with the hyperbola $S^2 = 4ab$. The possible trajectories in the (a, b) -plane are shown in figure 8. We distinguish two different regimes depending on the behaviour of z_m .

The finite region of motion in the (a, b) -plane corresponds to the periodic evolution of z_m . When $\Delta_{ab}^2 < 0$ (figure 8a, b) the motion is 'finite' regardless of the initial wave parameters (S, a_0, b_0) . The case of figure 8(c) is a special one as a wave can move along two different segments of the curve, depending on a_0 and b_0 (but not S). We distinguish this case because there are no similar transformation regimes in the model (4.7), where transformation is determined by parametric dependence on S only.

We note that z_m tends to infinity at the point $a = 0, b = 0$. This fact may be considered as a shortcoming of the model (4.7) and interpreted as follows. In the model

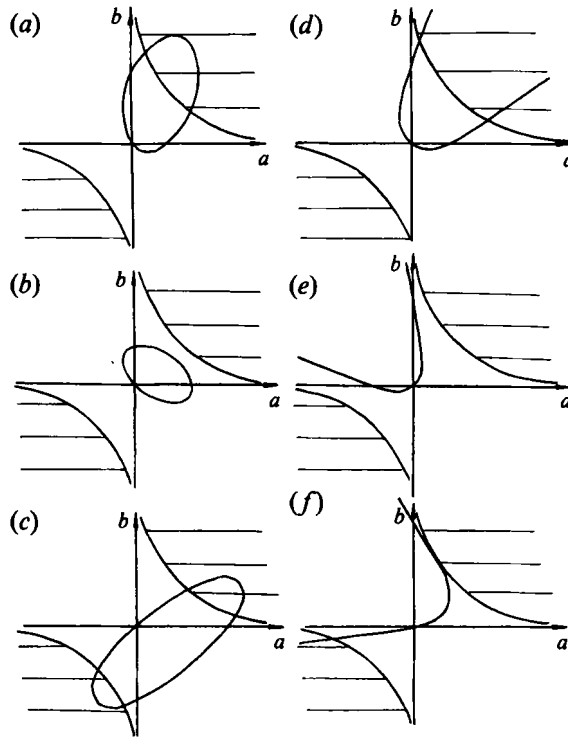


FIGURE 8. Short internal-wave trajectories in the model (4.1) in the (a, b) -plane depending on the mean-current field geometry (values of constant A, B, N, α, β) and wave-packet parameters (value of S). The hatched region is the non-transparency region where $S^2 < 4ab$ (i.e. $S^2 < 4k_0 l_0 x_0 y_0$). When $\omega(a, b) = \text{const}$ is an ellipse (a, b, c) $a(t)$ and $b(t)$ vary periodically with time (this does not mean that $x(t)$ or $k(t)$ are periodic functions). When $\omega(a, b) = \text{const}$ is a hyperbola, the situation when $|a|$ and $|b|$ grow infinitely is also possible (see e). It is easy to show that intersections of the curves $\omega(a, b) = \text{const}$ and $S^2 = 4ab$ give the simple reflection point where the reflection lasts a finite interval of time. Points where $\omega(a, b) = \text{const}$ is tangent to $S^2 = 4ab$ are reached asymptotically in an infinite time, (f).

(4.12) a particular ‘degenerate’ direction exists where there is no extremum of the current velocity which determines the short-wave propagation. It can also occur in the more general situation (4.1) as well and more than a single direction of ‘degeneracy’ may exist. In these cases wave propagation is determined by the density field guide or by density and current values at the ocean surface or bottom. In our model we have not taken into account these bounds on z_m . It does not appear to be of great importance as it can be shown that the wave achieves these critical points within a finite time. Moreover, trajectories exist which do not intersect the point $a = 0, b = 0$ (figure 8c).

When $\Delta_{ab}^2 > 0$ the evolution depends significantly on the initial wave parameters. Besides the case of figure 8(e) in which $\omega(a, b) = \text{const}$ and $S^2 = 4ab$ have no common points, the situation exists when both finite and infinite regimes are possible (figure 8f) depending on the initial values of a_0, b_0 .

We stress that all the criteria which determine whether a regime of transformation occurs are given by inequalities in terms of the initial wave parameters (by the number of points of intersections of $\omega_0(a, b) = \text{const}, S^2 = 4ab$). This means that effects related to the type of trajectory in the (a, b) -plane are structurally stable. In other words, the neighbour harmonics of the wave packet will evolve in a similar way. It should be

stressed in connection with the case presented in figure 8(*f*), that it takes infinite time for the packet to achieve the point of tangency of $S^2 = 4ab$ and $\omega_0 = \text{const}$. One should consider the situation of figure 8(*f'*) as structurally unstable.

4.4.2. Internal-wave kinematics in the model of dominant mean shear vertical inhomogeneity

The qualitative analysis of the behaviour of the depth of localization z_m presented above can easily be combined with the general properties of the model (4.1) which were considered in §4.2. This synthesis allows one to analyse the internal-wave kinematics in original variables and to preview the possible types of wave evolution. The case of the monotonic variation of a and b and, hence, relatively simple variation of z_m is of less interest as it does not differ principally from the case of the model of §3.2.

The most interesting dynamic regime occurs when z_m is changing periodically with time. The terms Δ_i are changing periodically as well. But the mean (over period) value $\int_t^{t+T} \Delta_i dt$ does not equal zero in general case. Hence there are no structurally stable periodic motions in original variables for the model under consideration. So, this model demonstrates fairly well one of the properties of the internal-wave dynamics in the general model (4.1).

Figure 7 shows sketches of the different possible types of internal-wave trajectory for the general model (4.1). The same picture holds for the model (4.12). The wave trajectories are more intricate than in §3. The reasons for reversibility of the motion in terms of changes in the angle variables are evident: the current at the different depths has different directions and the wave 'feels' it through changes in z_m .

Two principally different types of wave evolution can be distinguished depending on the sign of

$$\int_t^{t+T} \Delta_i dt < 0 \quad (i = 1, 2, 3, 4).$$

In the first one the wave trajectory twists in the (k, l) -plane and untwists in the (x, y) -plane (perhaps in limited range of angles). When our local analysis breaks down the WKB-approximation will become invalid as well while $|k| \rightarrow 0$.

In the second case all our approximations remain valid while $|k| \rightarrow \infty$ and $|x| \rightarrow 0$. The wave packet 'falls' into the point $x = 0$. It is easy to take into consideration intrinsic wave motion and to show the validity of local analysis in this case as well. We shall not dwell upon this here. While there is a range (in k, x)-space) of the wave initial conditions, where this 'falling' into the centre of eddy (4.1) takes place, we can say that a certain share of the internal-wave-field energy will be localized in the immediate vicinity of the eddy axis when t is sufficiently large.

Evidently, both horizontal and vertical inhomogeneities are taking part in the complication (relating to the case of §3) of trajectories. Thus, there is no sense in interrelations of elliptic trajectories in the model of §3 and spiral trajectories of the model under discussion, and new features of the short-wave evolution discussed above prompt us to introduce a new concept of 'spectral-spatial focusing' of an internal wave.

4.5. On the spectral-spatial focusing of internal waves due to trapping

We distinguish these two concepts (spectral and spatial focusing) on the basis of concepts that were introduced in §3. When $z_m = \text{const}$, different spectral components are generally trapped at different locations owing to the dispersive effects taking place. However, different trajectories with a fixed wave vector are focused along some curves, that is spatial focusing takes place.

To understand the spectral focusing mechanism we shall return to the analysis of §3.3. We have noted that the effect of spatial focusing of different harmonics at the same point is not the consequence of the 'degenerate' model only. We have obtained the same phenomenon in a non-solenoidal current velocity field in the two-layer-of-localization model of §4.2. This note allows us to sketch the following model for this mechanism.

While internal waves in the short-wave limit feel an 'effective' velocity field depending on z_m only, we can simplify our problem by reducing it to this two-dimensional velocity field. What are the specific features of this field? Let us calculate its derivatives, taking into account that z_m depends on x :

$$\frac{\partial U_{\text{eff}}}{\partial x_j} = \frac{\partial U(z_m, \mathbf{x})}{\partial x_j} + \frac{\partial U(z_m, \mathbf{x})}{\partial z_m} \frac{dz_m}{dx_j}.$$

For the divergence in the model (4.12) we have

$$\nabla_h \cdot U_{\text{eff}} = 2ab \frac{A^2 B^2 \alpha^2 \beta^2 h^2}{(\alpha^2 Aa + \beta^2 Bb)^3}. \quad (4.15)$$

By integrating (4.15) over a range of angles we can obtain the total flux for the waves of fixed intrinsic frequency from this angle range:

$$\bar{\nabla}_h^\varphi \cdot U_{\text{eff}} = \pi^{-1} A^3 B^2 \alpha^2 \beta^2 h^2 \int_{\varphi_1}^{\varphi_2} \frac{\sin \varphi \cos \varphi (\sin \varphi + \cos \varphi)}{(\alpha^2 A \cos \varphi + \beta^2 B \sin \varphi)^3} d\varphi. \quad (4.16)$$

We shall specify φ_1, φ_2 below.

Taking $\varphi_1 = 0, \varphi_2 = 2\pi$ we obtain an expression containing a singularity. The principal value of (4.16) does not equal zero in the general case. To avoid this integration and to make our model more realistic we shall confine the depth range and, thus, the integration range. Assume the fluid surface to be at $z = 0$ and the bottom at $z = H$. The depth z_m , consequently, varies from 0 to H . When $z_m = 0$ or $z_m = H$ and the velocity field is solenoidal, and then the divergence of the effective velocity field is zero in a certain range of angles. But the integral divergence (4.16), generally, does not equal zero. Its sign may be different and different types of wave evolution can occur: divergence or convergence of the wave trajectories such as in §§4.2 and 4.4 takes place.

We note that the divergence integral (4.16) does not depend on $|k|$ as we take the short-wave limit and allow vertical non-uniformity of the velocity to dominate absolutely. By taking into account density stratification it is easy to obtain the dependence of the divergence on $|k|$ even in the short-wave approximation. Then it can be shown that the efficiency of spectral and space focusing increases as $|k|$ increases.

As we have seen, a good understanding of these phenomena and, sometimes, some evaluations of its efficiency can be achieved by analysis of the two-layer-of-localization model. In such a model the divergence of the effective velocity field depends on the velocity discontinuity across the rays dividing the regions of different depths of localization.

4.6. Discussion

All the models considered above are particular cases of a more general model (4.1). The analysis of these particular cases was necessary in order to introduce some new concept, which are helpful for understanding the general problem.

We have established the dominating role of vertical inhomogeneity of the current in the kinematics and dynamics of internal waves. We have introduced and advanced the

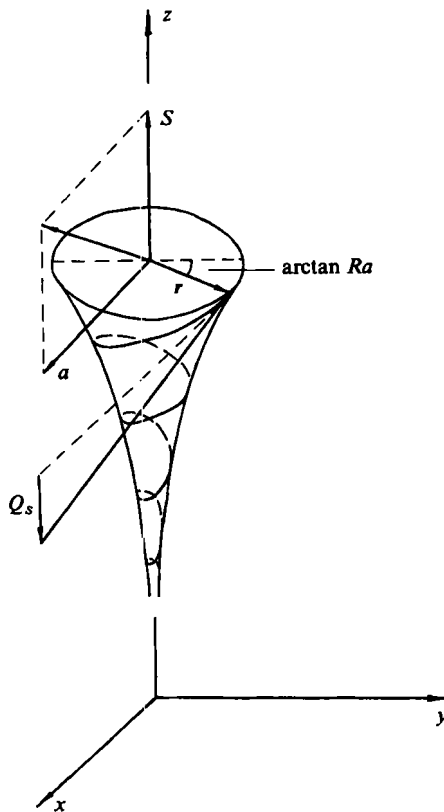


FIGURE 9. The analogy between the wave packet evolution (within the model (4.1)) and the classical particle motion in a potential field along a funnel-like surface. There are two first integrals of this motion: the energy of the particle (the sum of kinetic and potential energies) which is similar to the wave frequency ω , and the kinetic impulse projection which is like the integral S for an internal wave packet. The particle which falls into this 'funnel' is accelerated and tends infinitely to the point $x = 0$ like the internal-wave quasi-particle.

new concept of 'the depth of localization' z_m , depending on both the hydrophysical mean fields and the wave kinematical parameters (wave vectors). The depth of localization is a good physical concept which illustrates the transformation of a real three-dimensional velocity field into some family of two-dimensional 'effective velocity fields'. Each element of this family is determined by the initial wave parameters because of the dependence of z_m on k . Thus, the concept enables us to reformulate (to some extent) our original three-dimensional problem in terms of well-known problems of two-dimensional hydrodynamics. The specific features of this new problem lie in the dependence of the type of effective velocity field on the spatial variables, and in the parametric dependence of this field on the initial wave parameters. Even when the real velocity field is smooth and solenoidal, the effective current appears non-solenoidal and singular. The effective velocity singularities act similarly to the point sources and sinks in hydrodynamics.

We now elaborate on the above-mentioned analogy with the motion of classical particles in a potential field of a special type (figure 9). Consider a particle moving on a funnel-like surface in a common gravitational field. The vertical component of its kinetic momentum is conserved (an analogue of our first integral S). The particle has a radial component of velocity and its angle varies periodically with time (an analogue

of angle variable R_i). The depth of the particle (or its momentum Q_i) grows infinitely and the particle falls infinitely along the spiral-like trajectory. Variables a and b are kinetic momentum components, which vary periodically with time under gravitational force (an analogue of gyroscope precession).

This analogy gives us a new view on the internal-wave dynamics problem. The existence of 'funnels' for internal-wave-packet particles means specific irreversibility in a conservative system. We have got 'black holes', well-known in astrophysics, in a classical 'Internal-Wave Universe'. The singular surface of an infinite funnel corresponds to the singular effective velocity field in our problem. We stress that these singularities or 'holes' occur in generic situations with smooth ambient density and velocity fields and therefore the 'effective' mean flows should have a multi-hole-like structure.

5. Discussion and conclusions

A part of our programme, whose final goal is to find out the role of large-scale inhomogeneities of hydrophysical ocean fields in guided internal-wave dynamics has been realized in this paper. We have identified and investigated some generic mechanisms governing the evolution of internal waves in an inhomogeneous ocean, and some general tendencies of internal-wave evolution. This has been done using comparatively simple models.

A set of models which corresponds to the different types of vertical structure on the mean flows has been considered. It has been shown that different scenarios can occur depending on the type of inhomogeneity.

The main conclusion of our investigations is that: irreversible dynamical evolution of internal waves into small-scale horizontal and vertical ranges inevitably takes place under some very general assumptions about the structure of the ocean's hydrophysical fields and over a wide range of internal-wave parameters.

Moreover, the most intense internal-wave transformation by currents in many cases appears to occur mainly in horizontally and vertically strongly localized regions (because of wave packet 'gluing' to the mean current and the non-dispersive focusing of internal waves as mentioned above). This conclusion has many physical implications; for example, it permits us not only to simplify the mathematics of the problem (by exploiting the analogy with particle motion in a simple potential field), but as the problem reveals a conceptual resemblance with well-known problems of physics, these might help one in determining strategic directions of future investigation.

The main question for oceanic internal-wave investigators still remains the one formulated by Briscoe (1975): 'where does the internal wave energy come from, where does it go, and what happens to it along the way?' In this paper we have attempted to answer part of this question: what is the role of the internal-wave evolution tendencies discovered here in the internal-wave degeneration processes in the ocean? This question has an essential resemblance with the well-known astrophysical problem of 'black holes' as the 'substance devourer'.

Another analogy is the hydrodynamical one, which has been introduced on the basis of the model (4.1). The singularity of the effective velocity field connected with the phenomenon of trapping is similar to a well-known problem of hydrodynamics – the problem of point sources and sinks. Hence, a straightforward idea for further investigation is to construct these sources and sinks by transforming generic current and density fields, which internal wave kinematics depends on, into an effective current field U_{eff} . As the specific features of this transformation are investigated, the

hydrodynamical analogue should help us to develop our analysis for more general problems.

Another natural direction for further investigation is the extension to a higher order of approximation of the analysis of the ray equations (2.2), to consider the intrinsic motion of the internal wave packet. As wave-packet 'gluing' to the mean flow takes place it allows one to change to the transformed curvilinear coordinate system moving with the mean flow. This promises to be useful both for the analysis of local situations discussed above and for developing the 'non-local' analysis of trapping.

This is an outline of the most promising, from our point of view, avenues of further investigation of the effect of trapping within the same paradigm.

Our investigation has provided sufficient grounds to suppose the existence of a certain strong tendency for internal-wave-field evolution into the small-scale range. Now we certainly cannot specify quantitatively the importance of this tendency in internal-wave dynamics in the ocean. To answer this question we must come out of the framework of our models and, first of all, take nonlinearity into account. Work in this direction is in progress now.

The authors are grateful to G. Watson for his valuable comments on the first draft of the work. The hospitality of Royal Netherlands Meteorological Institute at De Bilt and l'Institut Mecanique Statistique de la Turbulence at Marseille (Luminy), where part of this work was done by one of the authors (V. I. Shrira), is appreciated.

Appendix A

There are four basic types of canonical transformations with S and a or b as canonical momenta:

$$\left. \begin{aligned} S_1 &= kx + ly, & Q_1 &= -\ln(k/p), \\ E_1 &= a = ky, & R_1 &= -l/k; \end{aligned} \right\} \quad (\text{A } 1)$$

$$\left. \begin{aligned} S_2 &= kx + ly, & Q_2 &= -\ln(l/p), \\ E_2 &= b = lx, & R_2 &= -k/l; \end{aligned} \right\} \quad (\text{A } 2)$$

$$\left. \begin{aligned} S_3 &= kx + ly, & Q_3 &= \ln(y/p), \\ E_3 &= a = ky, & R_3 &= x/y; \end{aligned} \right\} \quad (\text{A } 3)$$

$$\left. \begin{aligned} S_4 &= kx + ly, & Q_4 &= \ln(xp), \\ E_4 &= b = lx, & R_4 &= y/x. \end{aligned} \right\} \quad (\text{A } 4)$$

Here p is a constant chosen to make yp , k/p , xp , l/p dimensionless, S_i, E_i ($i = 1, 2, 3, 4$) are new canonical momenta, Q_i, R_i are canonically conjugated coordinates.

Appendix B

The explicit expression for the depth of localization z_m in the model (4.7) can easily be found from (4.2):

$$z_m = \frac{2(\alpha Aa + \beta Bb)}{\gamma(\omega - Aa - Bb + \alpha_1 Aaz + \beta_2 Bbz)}. \quad (\text{B } 1)$$

The dispersion relation is obtained from (2.10) in the form

$$N_0^2 - G^2 + g^2 = \frac{2n+1}{\sqrt{2}} N_0 G \gamma (1 - g^2/G^2)^{-\frac{1}{2}} (k^2 + l^2)^{-\frac{1}{2}},$$

where $G = \omega - Aa - Bb + \alpha Aaz_1 + \beta Bbz_2$, $g = \sqrt{2(\alpha Aa + \beta Bb)}/\gamma$.

The explicit expression for ω can be presented in the form of an expansion in inverse powers of $|k|$:

$$\left. \begin{aligned} \omega &= \omega_0(a, b) + \omega_1(k, x, l, y) + o(|k|^{-\frac{1}{2}}), \\ \omega_0 &= Aa + Bb - \alpha Aaz_1 - \beta Bbz_2 \pm \sqrt{2(\alpha Aa + \beta Bb)}/\gamma, \\ \omega_1 &= \pm \frac{(2n+1)^{\frac{3}{2}}}{2} \left[\frac{N^2 \gamma_0 (\alpha Aa + \beta Bb)}{\sqrt{2(k^2 + l^2)}} \right]^{-\frac{1}{2}}. \end{aligned} \right\} \quad (\text{B } 2)$$

Using (B 2) we get the short-wave asymptotes of (B 1):

$$z_m = \pm \frac{\sqrt{2}}{\gamma} \left[1 - \frac{(2n+1)^{\frac{3}{2}}}{2} \left(\frac{N^2 \gamma^4}{2(\alpha Aa + \beta Bb)^2 (k^2 + l^2)} \right)^{\frac{1}{2}} + o(|k|^{-\frac{1}{2}}) \right]. \quad (\text{B } 3)$$

Appendix C

According to definition (2.12) the maximal-over-depth value of the wave vertical velocity A (amplitude) can be written in the form

$$A^2 \sim [\omega - k \cdot U(z_m)]^3 / [N^2(z_m) d(z_m)], \quad (\text{C } 1)$$

where $[\omega - k \cdot U(z_m)]^3 \approx G^3(1 - g^2/G^2)^3$, $N^2(z_m) \approx N_0^2(1 - g^2/G^2)$,

$$d(z_m) = \frac{G^{\frac{1}{2}}(1 - g^2/G^2)^{\frac{3}{2}}}{N_0^2 \gamma^{\frac{1}{2}} (k^2 + l^2)^{\frac{1}{2}}}. \quad (\text{C } 3)$$

Quite similar to (3.6) we get for the case $\Delta_s^2 > 0$ the following asymptotes:

$$k \sim \exp(\Delta_s t); \quad l \sim \exp(\Delta_s t); \quad x \sim \exp(\Delta_s t); \quad y \sim \exp(\Delta_s t).$$

Then the parameters in (C 2), (C 3) can also be expressed in terms of t :

$$\begin{aligned} [\omega - k \cdot U(z_m)]^3 &\sim \text{const}, \quad N^2(z_m) \sim \exp(-2\Delta_s t), \quad d(z_m) \sim \exp(-\Delta_s t), \\ A^2 &\sim \exp(3\Delta_s t) \{ \partial(x, y) / \partial(\xi, t) \}^{-1}. \end{aligned} \quad (\text{C } 4)$$

In particular, the equality (C 1) can be rewritten

$$A^2 = \text{const } N(z_m) \left(\frac{\partial(x, y)}{\partial(\xi, t)} d(z_m) \right)^{-1} \sim \exp(\Delta_s t) \text{const} \left(\frac{\partial(x, y)}{\partial(\xi, t)} \right)^{-1}. \quad (\text{C } 5)$$

Appendix D

Consider the model

$$U = Ay(1 + \frac{1}{2}\alpha^2(z - z_1)^2), \quad V = Bx(1 + \frac{1}{2}\beta^2(z - z_2)^2), \quad N = N_0 = \text{const}. \quad (\text{D } 1)$$

Constants $A, B, |\alpha|, |\beta|$ have a similar sense as in (4.7) (α^2, β^2 can be negative). For the horizon of localization we get

$$z_m = (\alpha^2 Aaz_1 + \beta^2 Bbz_2) / (\alpha^2 Aa + \beta^2 Bb). \quad (\text{D } 2)$$

While dispersion relation is

$$N_0^2 - G_*^2 + g_* G_* = ((2n+1)/\sqrt{2})(2N_0^2 g_* + g_*^2 G_*)^{\frac{1}{2}} G_*^{\frac{1}{2}} \quad (\text{D } 3)$$

where

$$g_* = (\alpha^2 Aa + \beta^2 Bb)(k^2 + l^2)^{-1}, \quad G_* = \omega - Aa - Bb - ABabh^2(\alpha^2 Aa + \beta^2 Bb)^{-1},$$

From (D 3) we obtain

$$h^2 = \frac{1}{2}\alpha^2\beta^2(z_1 - z_2)^2.$$

$$\omega = \omega_0(a, b) + \omega_1(k, x) + o(|k|^{-\frac{1}{2}}),$$

$$\omega_0 = \pm N_0 + Aa + Bb + ABabh^2(\alpha^2 Aa + \beta^2 Bb)^{-1}, \quad (\text{D } 4)$$

$$\omega_1 = \pm(n + \frac{1}{2})N_0^{\frac{1}{2}}(\alpha^2 Aa + \beta^2 Bb)^{\frac{1}{2}}(k^2 + l^2)^{-\frac{1}{2}}.$$

We emphasize that ω_1 tends to zero as $|k|^{-\frac{1}{2}}$, while in the previous case $\omega_1 \sim |k|^{-\frac{1}{2}}$. Short-wave asymptotic (D 4) corresponds to the structurally stable case (Borovikov & Levchenko 1987) in contrast to the intermediate asymptotics of the model (4.7).

REFERENCES

- ABRAMOVITZ, M. & STEGUN, I. A. (eds) 1964 *Handbook of Mathematical Functions*. US Govt. Printing Office.
- BADULIN, S. I. & SHRIRA, V. I. 1985 The trapping of internal waves by horizontally inhomogeneous currents of arbitrary geometry. *Izv. Akad. Nauk SSSR, Fiz. Atmos. Okeana* **21**, 982–992.
- BADULIN, S. I. & SHRIRA, V. I. 1993 On the irreversibility of inertial-wave dynamics due to wave trapping by mean flow inhomogeneities. Part 2.
- BADULIN, S. I., SHRIRA, V. I. & TSIMRING, L. SH. 1985 The trapping and vertical focusing of internal waves in a pycnocline due to the horizontal inhomogeneities of density and currents. *J. Fluid Mech.* **158**, 199–218 (referred to herein as BST2).
- BADULIN, S. I., TSIMRING, L. SH. & SHRIRA, V. I., 1983 On the trapping and vertical focusing of internal waves in a pycnocline due to the horizontal inhomogeneities of stratification and current. *Dokl. Acad. Nauk SSSR* **273**, 459–463 (referred to herein as BST1).
- BADULIN, S. I., VASILENKO, V. M. & GOLENKO, N. N. 1990 Transformation of internal waves in the equatorial Lomonosov current. *Izv. Akad. Nauk SSSR, Fiz. Atmos. Okeana* **26**, 279–289.
- BASOVICH, A. YA. & TSIMRING, L. SH. 1984 Internal waves in horizontally inhomogeneous flows. *J. Fluid Mech.* **142**, 233–249.
- BRISCOE, M. G. 1975 Introduction to collection of papers on oceanic internal waves. *J. Geophys. Res.* **80**, 289–290.
- BOOKER, J. R. & BRETHERTON, F. P. 1967 The critical layer for internal gravity waves in a shear flow. *J. Fluid Mech.* **27**, 513–539.
- BOROVIKOV, V. A. 1988 Critical layer formation in a stratified fluid with mean currents. *Reprint* N309. Instut Problem Mehaniki AN SSSR, Moscow 58p (in Russian).
- BOROVIKOV, V. A. & LEVCHENKO, E. S. 1987 The Green's functions of the internal wave equation in the layer of stratified fluid with average shear flows. *Morsk. Gidrofiz. J.* **1**, 24–32.
- BROUTMAN, D. 1986 On internal wave caustics. *J. Phys. Oceanogr.* **16**, 1625–1635.
- BROUTMAN, D. & GRIMSHAW, R. 1988 The energetics of the interaction between short small-amplitude internal waves. *J. Fluid Mech.* **196**, 93–106.
- BUNIMOVICH, L. A. & ZHMUR, V. V. 1986 Internal waves scattering in a horizontally inhomogeneous ocean. *Dokl. Acad. Nauk SSSR* **286**, 197–200.
- CRAIK, A. D. 1989 The stability of unbounded two- and three-dimensional flows subject to body forces: some exact solutions. *J. Fluid Mech.* **198**, 275–292.
- CRAIK, A. D. & CRIMINALE, W. O. 1986 Evolution of wave-like disturbances in shear flows: A class of exact solutions of the Navier–Stokes equations. *Proc. R. Soc. Lond. A* **406**, 13–26.
- EROKHIN, N. S. & SAGDEEV, R. Z. 1985a On the theory of anomalous focusing of internal waves in a two-dimensional nonuniform fluid. Part 1. A stationary problem. *Morsk. Gidrofiz. J.* **2**, 15–27.
- EROKHIN, N. S. & SAGDEEV, R. Z. 1985b On the theory of anomalous focusing of internal waves in a horizontally inhomogeneous fluid. Part 2. Precise solution of the two-dimensional problem with regard to viscosity nonstationarity. *Morsk. Gidrofiz. J.* **4**, 3–10.
- JONES, W. L. 1969 Ray tracing for internal gravity waves. *J. Geophys. Res.* **74**, 2028–2033.

- LEBLOND, P. H. & MYSAK, L. A. 1979 *Waves in the Ocean*. Elsevier.
- LEVINE, M. D. 1983 Internal waves in the ocean: a review. *Rev. Geophys. Space Phys.* **21**, 1206–1216.
- MCCOMAS, C. H. & BRETHERTON, F. D. 1977 Resonant interactions of the oceanic internal wave field. *J. Phys. Oceanogr.* **7**, 836–845.
- MCCOMAS, C. H. & MÜLLER, P. 1981 The dynamic balance of internal waves. *J. Phys. Oceanogr.* **11**, 970–986.
- MIROPOLSKY, YU. Z. 1981 *Dynamics of Internal Gravity Waves in the Ocean*. Leningrad: Gidrometeoizdat.
- OLBERS, D. 1981 The propagation of internal waves in a geostrophic current. *J. Phys. Oceanogr.* **11**, 1224–1230.
- OLBERS, D. J. 1983 Models of the oceanic internal wave field. *Rev. Geophys. Space Phys.* **21**, 1567–1606.
- RAEVSKY, M. A. 1983 On the propagation of gravity waves in randomly inhomogeneous currents. *Izv. Acad. Nauk SSSR. Fiz. Atmos. Okeana* **19**, 639–645.
- VORONOVICH, A. G. 1976 The propagation of surface and internal gravity waves in the geometric optics approach. *Izv. Akad. Nauk SSSR, Fiz. Atmos. Okeana* **12**, 850–857.
- WATSON, K. M. 1985 Interaction between internal waves and mesoscale flow. *J. Phys. Oceanogr.* **15**, 1296–1311.